FDR4ALT

Validation Report Document
Ocean & Coastal TDP

CLS-ENV-NT-23-0427

Issue 5.0 – 04/07/2023

Public

AUTHORS TABLE

Object	Name
Authors	Hélène Roinard (CLS), Fernando Nino (LEGOS), Fanny Piras (CLS)
Checked by	Gabriele Brizzi (SERCO) and Pierre Féménias (ESA)
Accepted by	Pierre Féménias (ESA)

CHRONOLOGY ISSUES

Issue	Date	Object
1.0	17/05/22	Draft version for Phase 2 PM#1
2.0	02/12/22	Intermediate version for Phase 2 PM #1 (80% completed for ENVISAT)
3.0	02/05/23	Final version for Final Review
4.0	23/05/23	Final version for Final Review with RIDs implemented
5.0	04/07/23	Updated version with ERS-1 results + document separated into distinct reports

TABLE OF CONTENT

LIST OF FIGURES

LIST OF TABLES

1 Introduction

This document has been written in the frame of the FDR4ALT project, ESA contract N°4000128220/19/I-BG. It is a deliverable of task 4 of the project and is identified as [D-4-02].

1.1 The FDR4ALT Project

In the framework of the European Long Term Data Preservation Program (LTDP+) which aims at generating innovative Earth system data records named Fundamental Data Records (basically level 1 altimeter and radiometer data) and Thematic Data Records (basically level 2+ geophysical products), ESA/ESRIN has launched a reprocessing activity of ERS-1, ERS-2 and ENVISAT altimeter and radiometer dataset, called the FDR4ALT project (Fundamental Data Records for Altimetry). A large consortium of thematic experts has been formed to perform these activities which are:

1) To define products including the long, harmonized record of uncertainty-quantified observations.

2) To define the most appropriate level 1 and level 2 processing.

3) To reprocess the whole times series according to the predefined processing.

4) To validate the different products and provide them to large communities of users focused on the observation of the atmosphere, ocean topography, ocean waves, coastal, hydrology, sea ice, ice sheet regions.

1.2 Purpose and scope of the validation report

After the FDR/TDP definition step and all benchmarking (Round Robin) between standard solutions addressed by each expert group, comes the production and validation step.

The objective of this document is to provide a validation report for the Ocean & Coastal TDP, following the strategy defined in the Validation Plan Document [D-4-01]. Note that to avoid heavy documents, the validation reports have been divided: there is one validation report for the FDRs (ALT FDR and MWR FDR) and one validation for each of the six TDPs. This document therefore contains only results for the **Ocean & Coastal TDP**.

This document describes in detail the validation that has been performed for the Ocean & Coastal TDP to assess the performances of the FDR4ALT final products. The validation covers the full lifespan of the missions and therefore includes long-term analysis, as well as cyclic analysis or targeted analysis that are relevant for this TDP.

2 Terminology

This section aims at defining clearly the terminology used in the FDR4ALT deliverables.

- **Product** refers a specific type of file, defined and described by a dedicated handbook, and designed for a clear purpose (the FDR4ALT project, the REAPER project, …). It is a "container". One product refers to one file. The use of plural is designed to refer to a group of files, for instance the Thematic Data Products. "FDR4ALT products" will usually refer to all TDPs and FDRs, i.e., the outputs of the whole project. Note that the word "product" does not imply any notion of start date or end date, whereas "dataset" does.
- **File** can be used to refer to one single product or any other file that is not a product.
- **Parameter or variable** refers to a product's field, i.e., the content of the product. For instance, the sea level anomaly is a parameter of the Ocean & Coastal Thematic Data Products.
  Dataset can be used to refer to any group of data, not necessarily products. However, in the context of this project, it will often be used to refer to a sub-ensemble of products, on a specific period of time or a specific geographic area. For instance, the TDS (test dataset) refers to a dataset of 3 years of test products.

3 Ocean & Coastal Topography Thematic Data Products

3.1 Introduction

The validation of the Ocean and Coastal Topography TDP follows a simple two-phase plan: pre-validation of the products according to the analysis of selected test zones, and statistical validation of the global product. We will first describe the validation approach and then show the validation results.

In most cases, we separate results for phase B (cycles 6 to 94) and phase C (cycles 95-113) of ENVISAT.

In this section, the coastal validation and the global ocean validation are divided into two distinct sections.

3.2 Coastal TDP: ENVISAT and ERS

Five validations zones have been selected for an in-depth analysis of the TDP coastal product:

- Mediterranean Sea
- Northeast Atlantic
- European Arctic
- Eastern North America
- Eastern Australia

The choice of these regions was made by taking into account their diversity of oceanographic contexts, and the availability of tide gauge data compatible with the ERS and ENVISAT missions timespan.

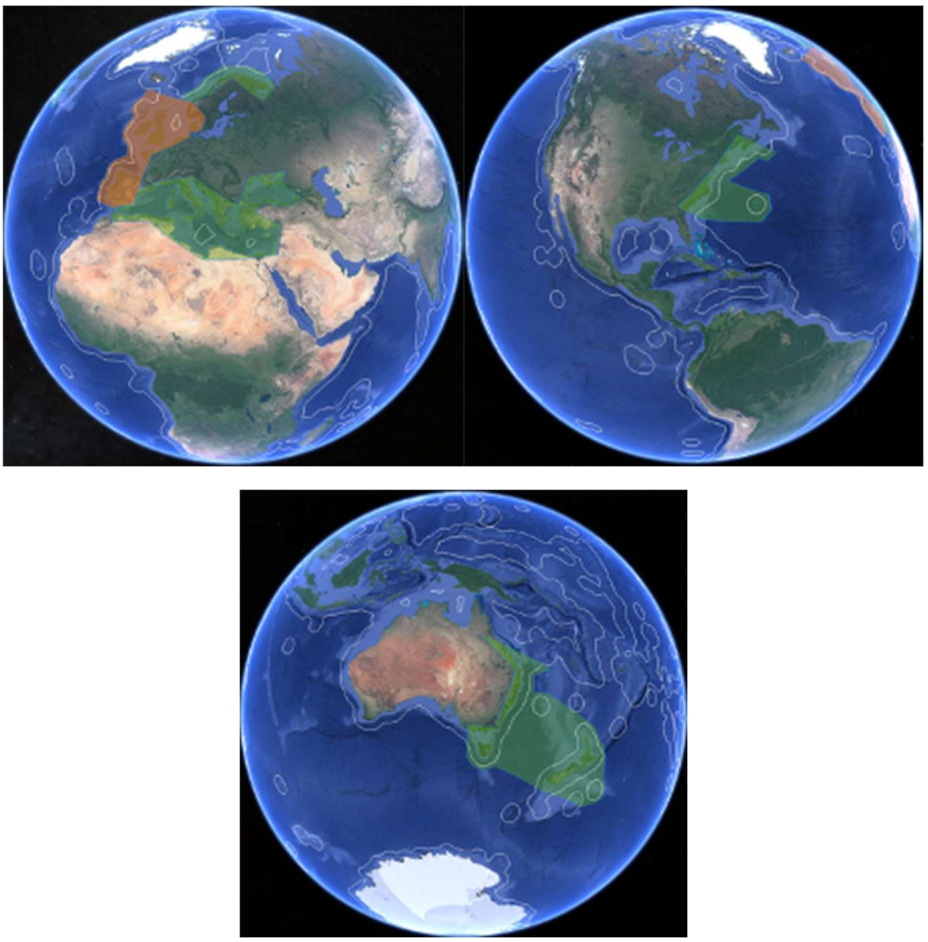

Figure 1 - Location of Coastal Validation Zones. (Top left): Mediterranean, North East Atlantic and European Arctic. (Top right) Eastern North America and (Bottom) Eastern Australia

The validation task is done at two levels:

- Using L2 data the statistical properties of the L2 coastal product are assessed.
- Using time series (L3 data) obtained with the coastal X-TRACK processing chain, we validate continuity and tide gauge correlation quality.

The full analysis presented here includes:

- statistical characterization and analysis of SSH, range and all corrections
- tandem flight period analysis
- regional crossover analysis on MSSH, sigma 0, and SSB, with particular attention to the evolution of cross-over statistics as a function of distance to the coast.
- tide gauge correlation with altimetry using Taylor diagrams for ENVISAT and ERS-2. ERS-1 has not sufficiently long timeseries to correlate accurately with tide gauge data.
- continuity analysis between open ocean and coastal zone

For the statistical characterization of corrections, we will analyse evolution through time and space. We will define criteria for detecting outliers in temporal variation for a given region using the distance to the coast as a parameter. The statistical distribution using a kernel density estimator will also be used to identify any anomalous behaviour. For spatial variations, outlier detection will be made using the difference to nearest neighbours, and map-based analysis on the relevant altimetric parameters.

Particularly interesting will also be the tandem flight period between ERS-2 and ENVISAT when they flew only 30 minutes apart (June 2002 to July 2003), and where inter-mission calibration can be done and where we expect very high correlation of the geophysical measurements of both missions.

We present here the analysis of validation of the five validation zones. For each zone we will show maps with the distribution of the mean sea surface height values, the distribution of valid points for the ocean_tide solutions, wet tropospheric correction and SLA. Also, we will present the along-track assessment of the SLA, as a function of distance to the coast twice: in the 0-200km and zooming into the 0-50km region.

3.2.1 Global completeness

A synthetic view of the completeness status of processing is given by plotting a matrix of cycles vs tracks. As such, each individual cell of the matrix represents one particular track in one particular cycle. The simples plot is that of an individual correction. We choose to show the LATITUDE, which is not a particular correction but a base attribute which exists when data is available. This will be our reference, and we will show either standalone corrections (like range, or WTC) or *percentage of available data relative to LATITUDE.*

For each particular data point, we will be plotting available data (or % relative to latitude), as seen in a region of less than 50km from the coast (as measured from the distance_to_coast parameter from the GSHHG dataset).

ENVISAT

For ENVISAT, the reference data (LATITUDE) shows the absolute number of available high rate (20hz) data points and with them we can easily see the missing tracks/cycles. As seen in the figures below, the overall

impression is the same, but there is a big loss in the raw WTC data (before coastal edition), as seen in the absolute number of available data points (up to 8000 in latitude, but only up to 4000 in WTC).

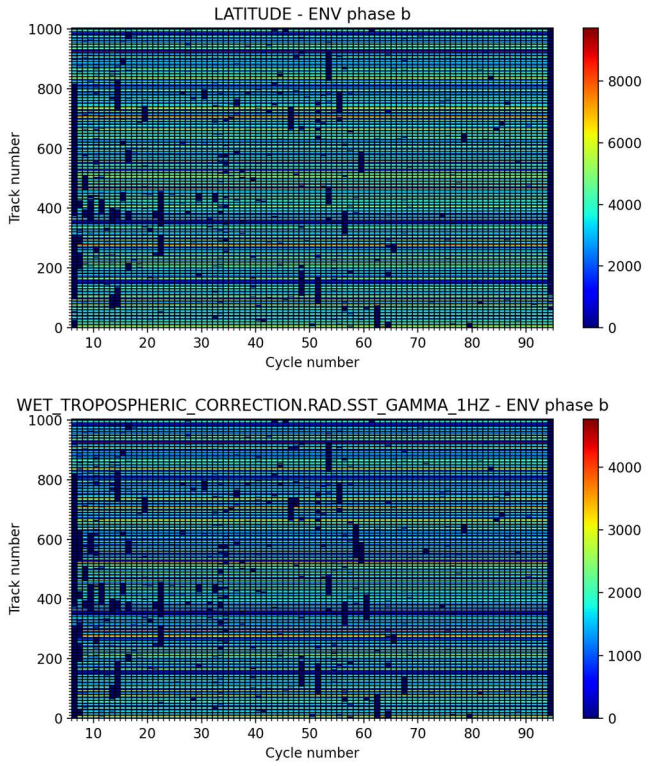

When looking at the percentage of available data relative to the data present (as given by the LATITUDE variable), the adaptive retracking RANGE has very high scores near 100% (missing data are seen as white

"holes" in the plot). Some tracks show very low raw WTC availability (as track 600 on cycle 58) despite being present for RANGE.

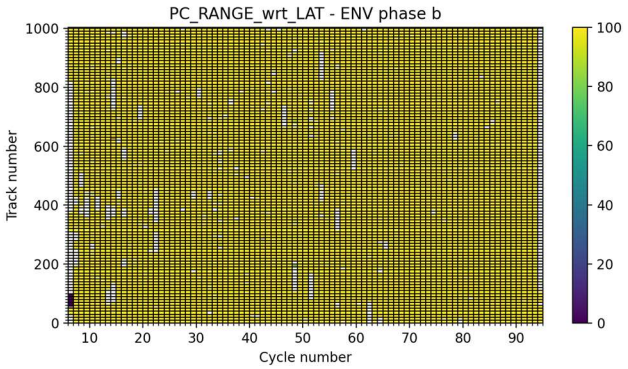

When looking at the coastal Sea Level Anomaly (SLA) we clearly see the SLA patterns follows that of the edited WTC.

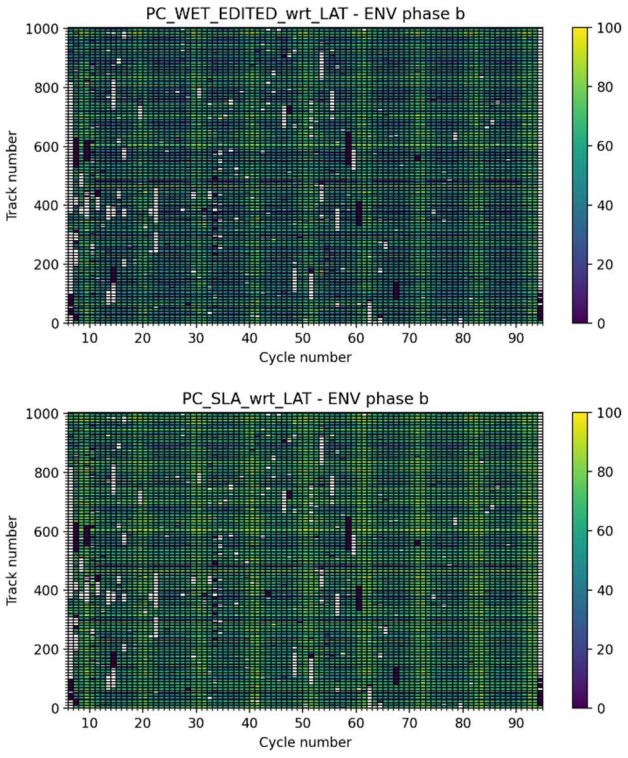

The stripes that appear on the SLA completeness plot make visible the different seasonality of GPD+ data and WTC. We see that at slightly over 10 cycles (~1 year) a bright yellow stripe becomes visible showing that periodically the GPD and the WTC tend to agree more, rejecting less coastal data. The stripes are more visible if data is restricted to a narrower coastal band (e.g. 20km) and less visible if it is wider (e.g. 200km). But this is an artifact of the algorithm implemented to edit WTC (described on the DPM document, OCOTDP_WTC_EDITED section).

To have a better view of what is going on, we plotted the GPD+ and the WTC radiometer data along a time axis from 1996 to 2009 for ERS-2 and ENVISAT. We can clearly see an annual signal which is present in the GPD+ data and not in the WTC.

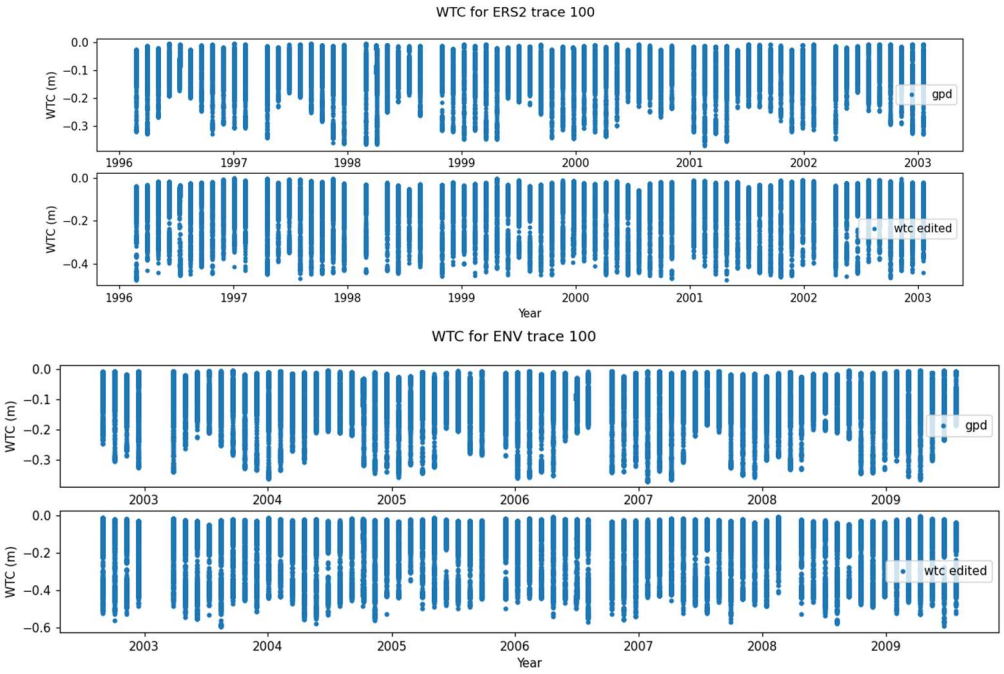

Because the GPD+ tropospheric correction has been cross-calibrated with the SSM/I mission and also uses GNSS data and is compatible with long-term trends, we believe that GPD+ has a better qualitative behaviour,

even if the absolute values of the new radiometer WTC are of much better quality than those used for the original calculation of the GPD+ correction.

As such, we believe the overall quality of the TDP coastal product is hindered by the quality of the WTC very near the coasts.

ENVISAT Phase C

Exhibits an overall good behaviour. The timeseries length being not so long, the annual stripes visible on ENVISAT and ERS-2 are not clearly visible here.

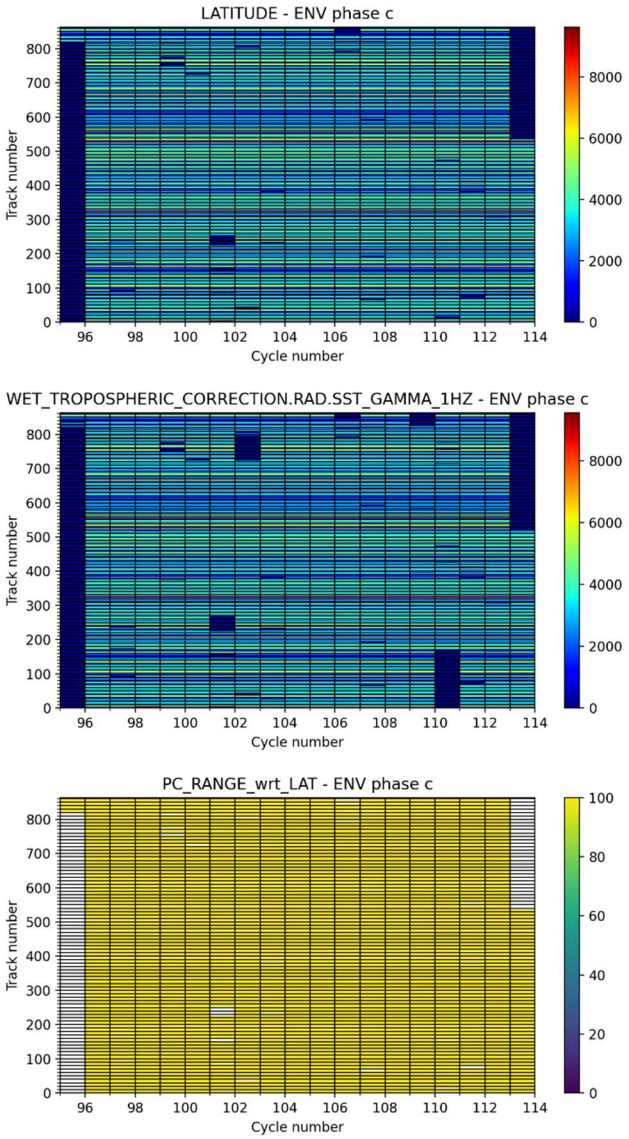

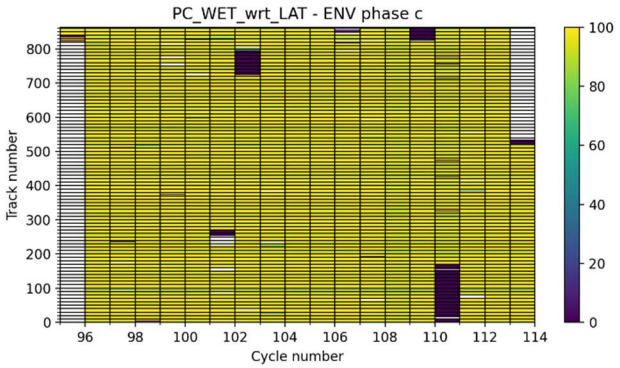

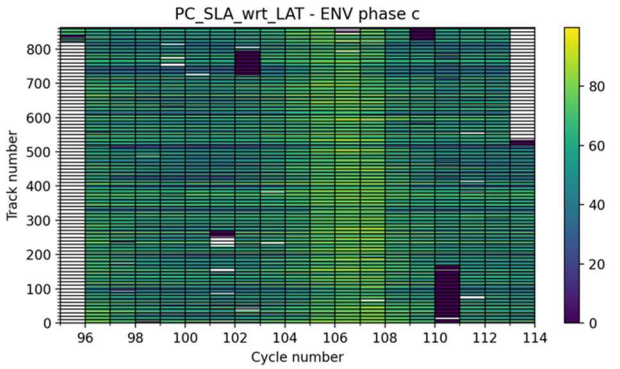

ERS-2

The same analysis is carried out for ERS-2 and is shown below. We immediately see that cycles 28 to 32 have many missing points.

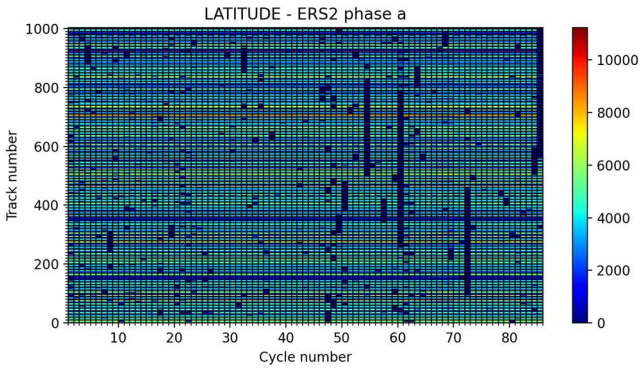

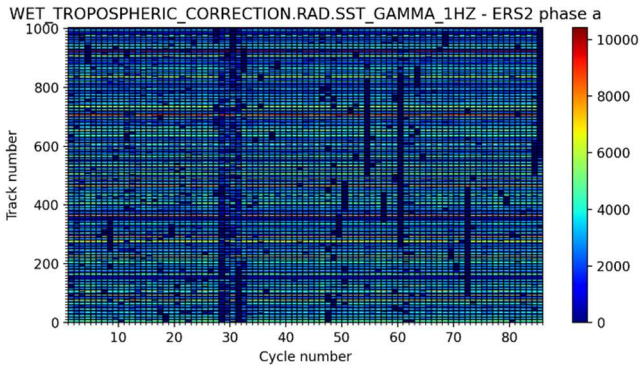

This missing data issue appears then on the computed SLA.

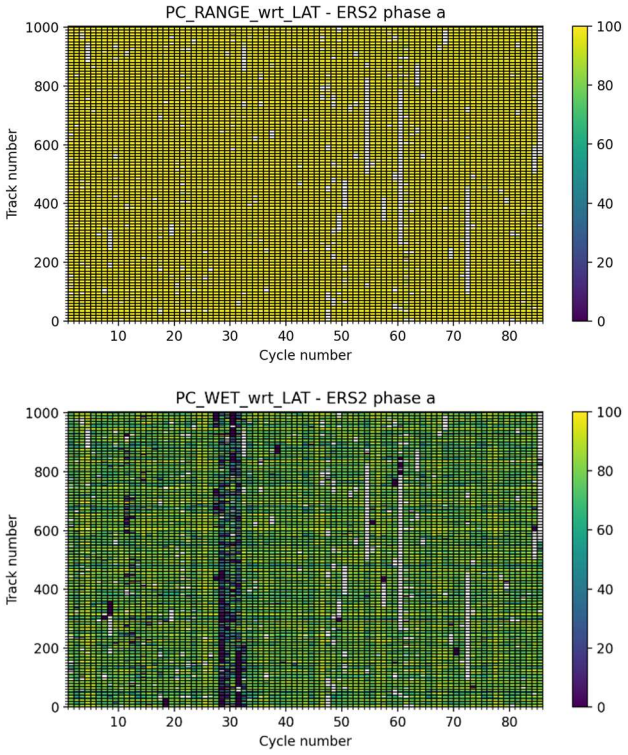

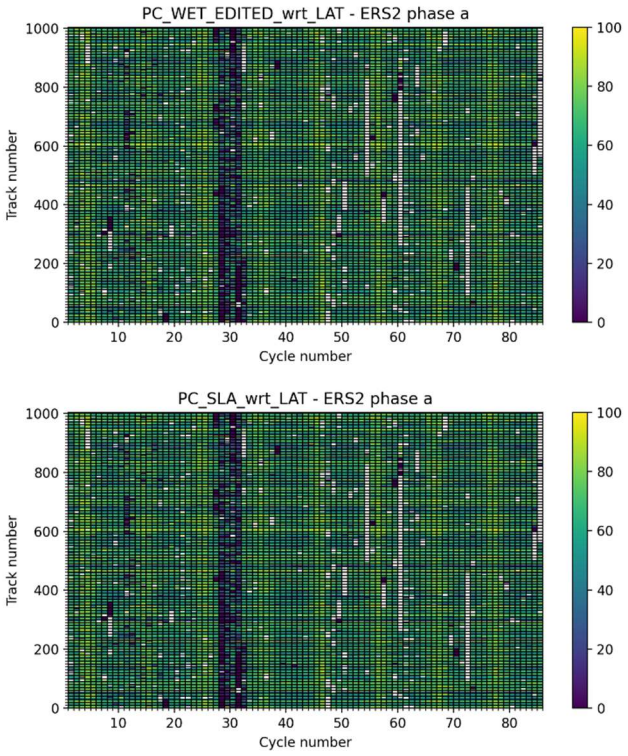

WTC behaviour near the coast

To finish this overview of completeness, we go back to the behaviour of the WTC near the coast. If we zoom on a map and look at a particular cycle (e.g., cycle 24) on a particular region, we see the huge difference between the radiometer WTC and the GPD+ correction.

On the Mediterranean Sea, the radiometer WTC shows outliers on many points near the coast as shown below, but none of this happens when using the GPD+ which appears very continuous.

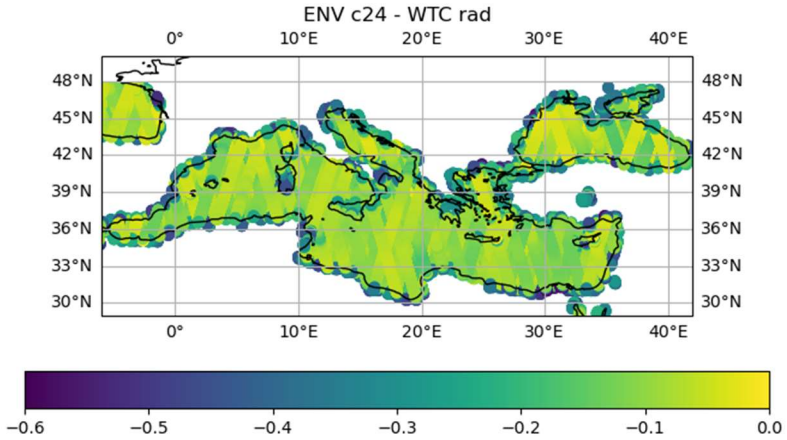

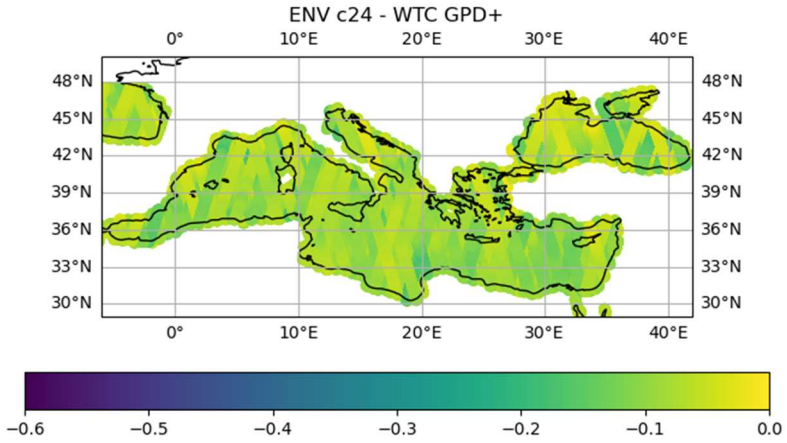

The same observation is made elsewhere, for example for the China Sea

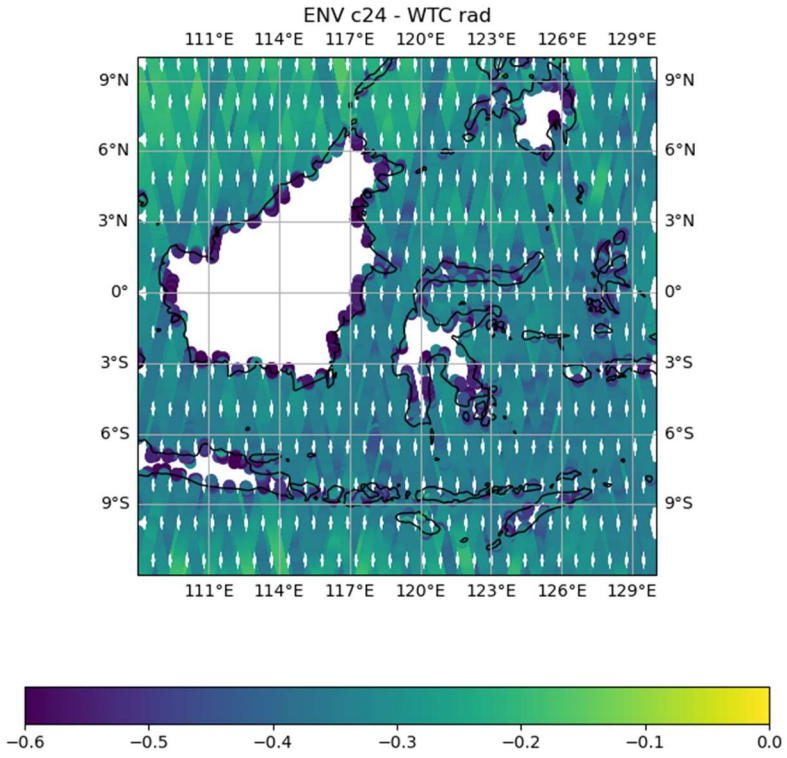

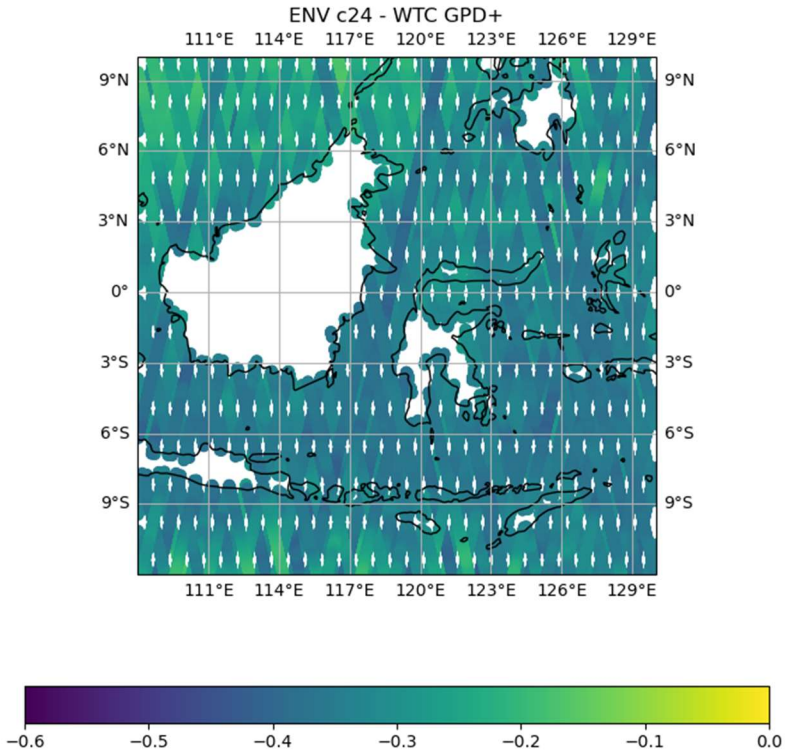

3.2.2 Mediterranean Sea

In the Mediterranean region, the visualisation of the number of valid points reveals some tracks with low number of points, but it is normal and consistent with the available data.

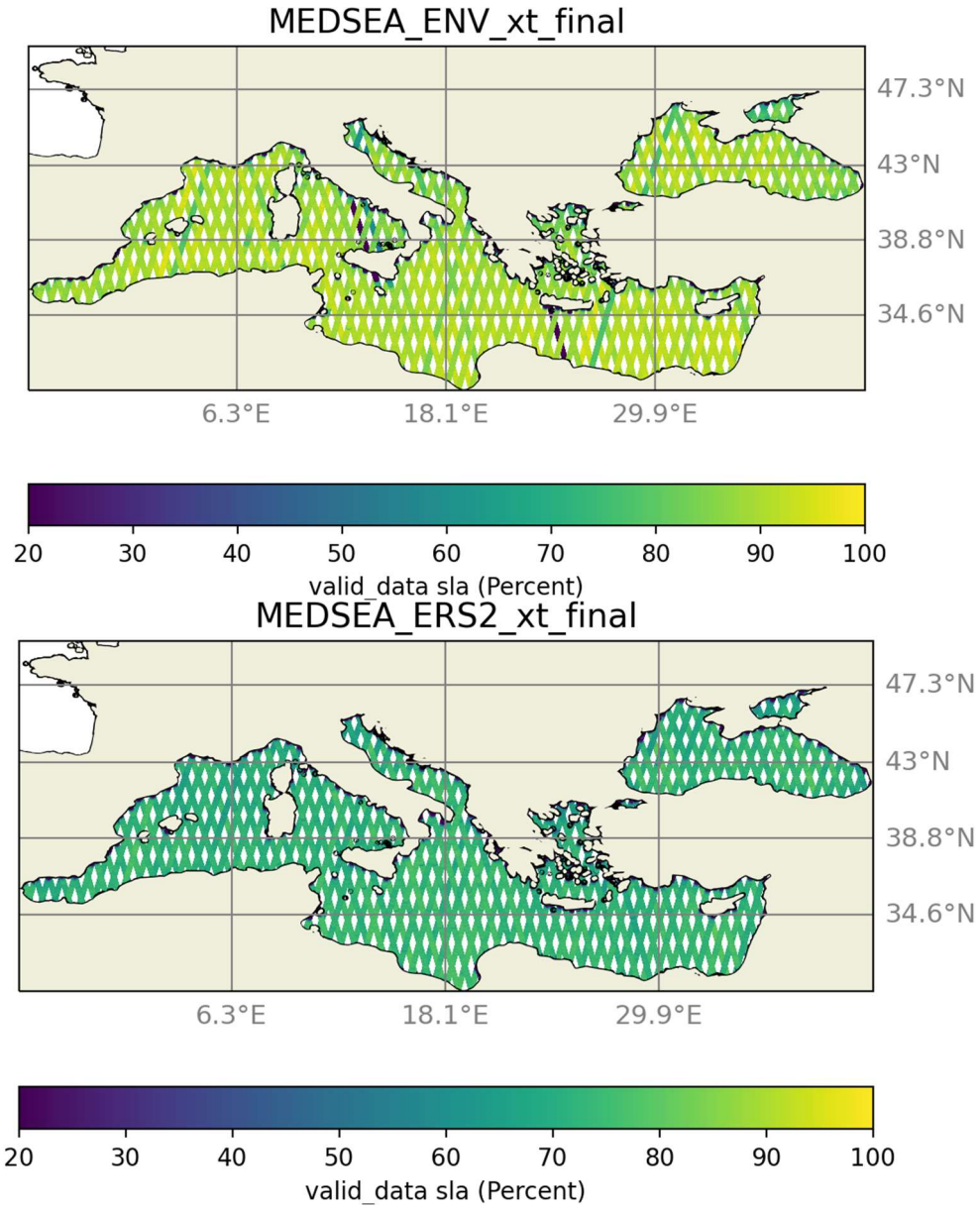

Figure 2 : Percentage of SLA valid data in the MedSea region for ENV (top),and ERS-2 (bottom).

For ENV, the statistics of SLA show a drop in valid data near the coast, just as expected. Its standard deviation goes up near the coast, closer than 7 km, and the number of valid points decreases at the same time, in line with what we have already seen for the Adaptive retracker which has been choses for this product. The behaviour of ERS-2 is different, since it uses the MLE3 retracker. Much more points are lost and there is a higher dispersion in range values. The number of valid data is much lower, even far from the coast (ca. 70% for ERS-2 and 90% for ENV).

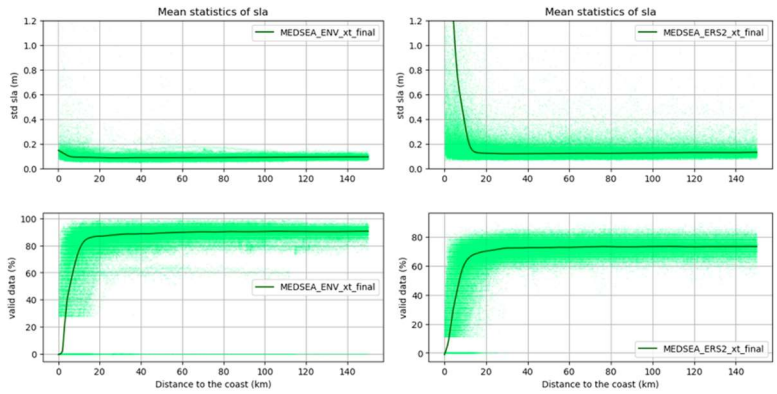

Figure 3 : Percentage of along-track valid data for SLA(ENV, left and ERS-2 right) in the MedSea region

3.2.2.1 Tide gauge analysis for Port Vendres

In this and all subsequent analysis of timeseries data and tide gauge coherency analysis, we used the coastal TDP to construct *a level 3* product, in which the data is reprojected onto a reference track to construct a time series. For the Mediterranean Sea we show two tide gauges: Port Vendres (in the Gulf of Lion) and Nice (SouthEastern french coast).

The figures below show the position of the tide gauge relative to the altimetry track, and a Taylor diagram showing the correlation and standard deviation of the altimetry timeseries relative to the tide gauge. For Port Vendres there is a 0.8 correlation on ENV timeseries which is very good, as we can see on the plot of the timeseries below. ERS-2 exhibits a less good correlation, though at 0.7 is still good. A table summarizes the statistical properties of points *common to both the tide gauges and the altimetry time series* (i.e., observed at the same time) for each mission considered.

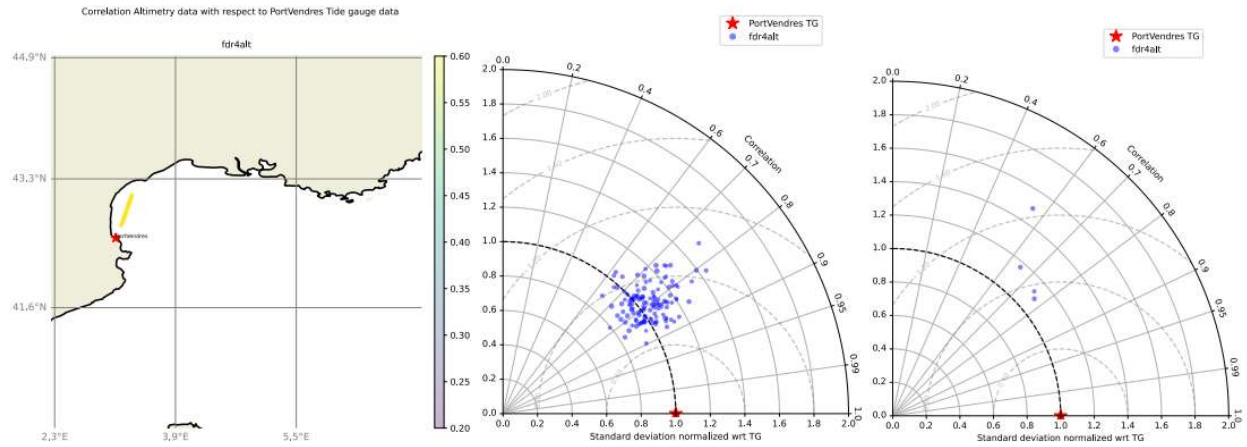

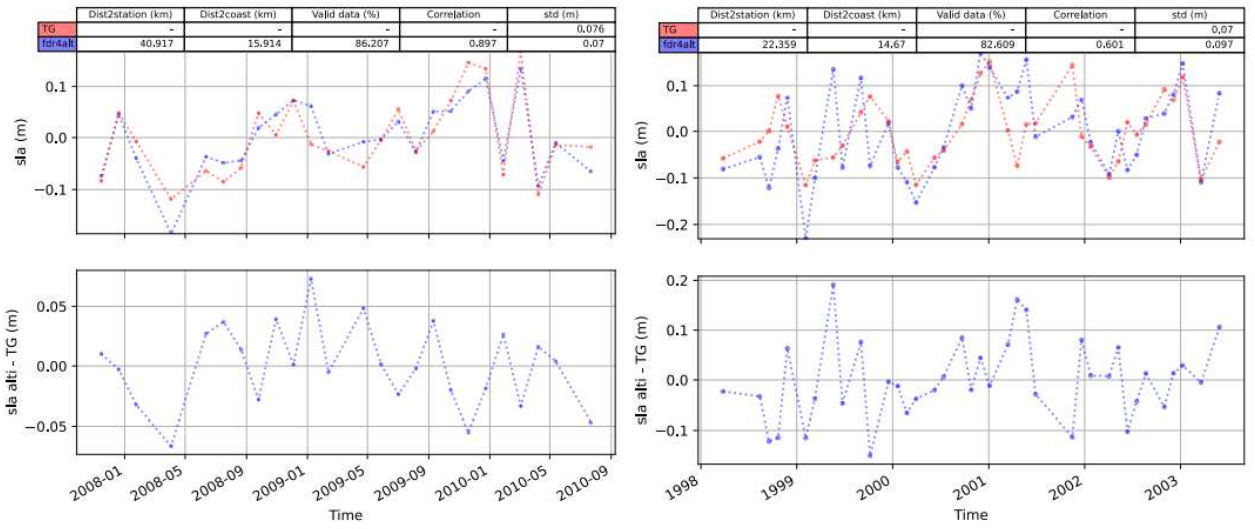

ENV ERS-2

ENV

Product	Valid data (%)	Correlation	std (m)	rmsd (m)
fdr4alt	91.352	0.789	0.078	0.05

ERS-2

Product	Valid data (%)	Correlation	std (m)	rmsd (m)
fdr4alt	96.591	0.682	0.122	0.091

Figure 4 : Location of the Port Vendres tide gauge in the french Mediterranean coast, with colormap of the correlation of each point (top, left). The Taylor diagram for all altimetry timeseries is plotted with respect to the tide gauge (for ENV top center, and ERS-2 top right). The middle panel shows the timeseries themselves for the point with best correlation (blue) and the tide gauge (red, left for ENV and right for ERS-2). The bottom panel shows tabular statistics for summarizing the behaviour for ENV and ERS-2.

3.2.2.2 Tide gauge analysis for Nice

This particular site has a track that arrives perpendicular to the coast and is thus in the most favorable geometrical condition for a coastal analysis (land contamination arrives in a predictable manner). However, the tide gauge is several tens of km far from the track and on a coast with an angle with respect to the general coastal line. The correlation for ENV is good and shows the FDR4ALT is making a good job on coastal data. On the other hand, ERS-2 performance is below par and other diagnostic reports don't show anything abnormal on any correction, except the higher dispersion and lower quality of the retracker solution (MLE3 vs Adaptive retracker).

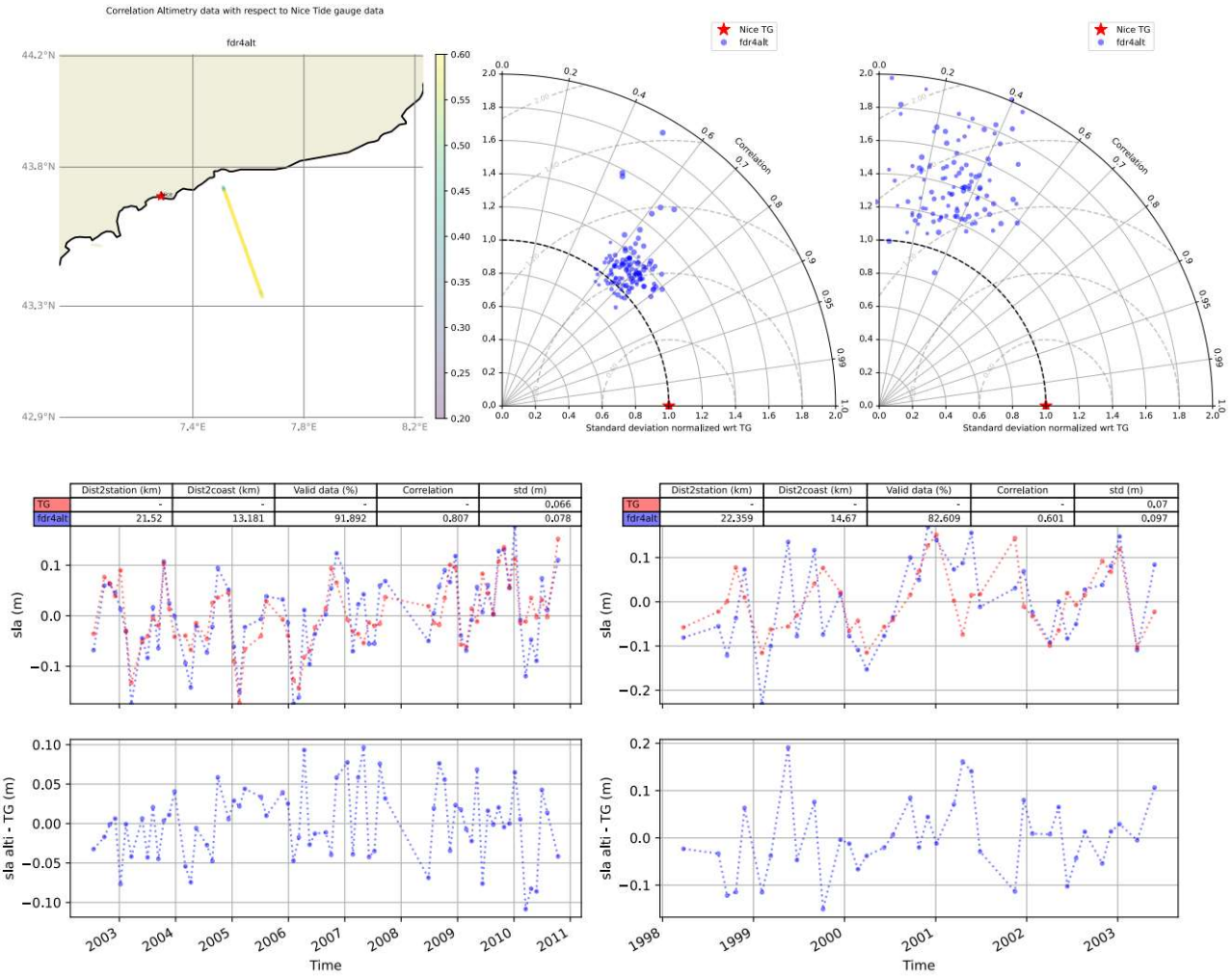

ENV ERS-2

ENV

Product	Valid data (%)	Correlation	std (m)	rmsd (m)
fdr4alt	92.28	0.671	0.33	0.313

ERS-2

Product	Valid data (%)	Correlation	std (m)	rmsd (m)
fdr4alt	79.822	0.295	0.109	0.112

Figure 5 : Location of the Nice tide gauge in the french Mediterranean coast, with colormap of the correlation of each point (top, left). The Taylor diagram for all altimetry timeseries is plotted with respect to the tide gauge (for ENV top center, and ERS-2 top right). The middle panel shows the timeseries themselves for the point with best correlation (blue) and the tide gauge (red, left for ENV and right for ERS-2). The bottom panel shows tabular statistics for summarizing the behaviour for ENV and ERS-2.

3.2.3 Northeast Atlantic

There is a dark patch on the maps below that can safely be ignored; the limits of the region are covered with the green values on the ocean tide map below.

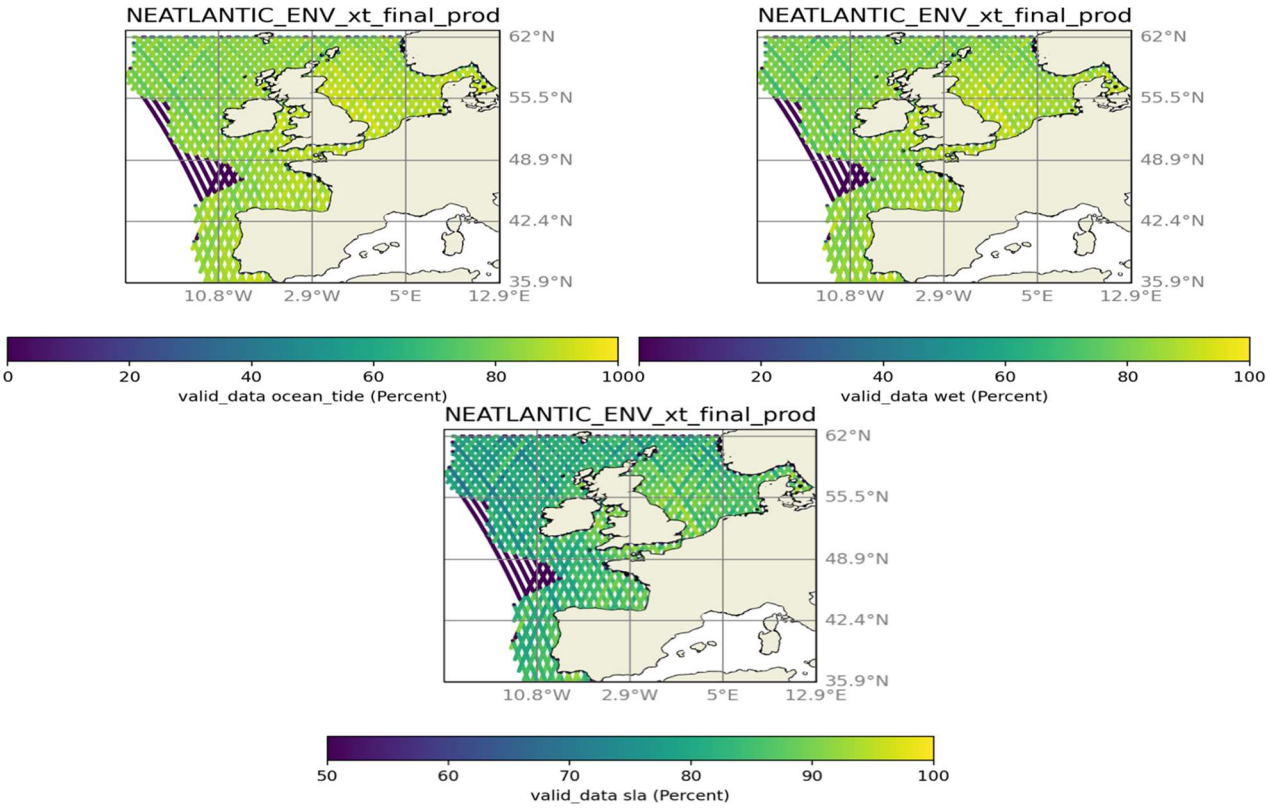

Figure 6 : Percentage of valid data in the North East Atlantic region for tide (top left), WTC (top right) and SLA (bottom)

The statistics of SLA are very good although the tides are not always very well represented in this zone. This is the effect of using the regional solution to the ocean tide, with unstructured grids.

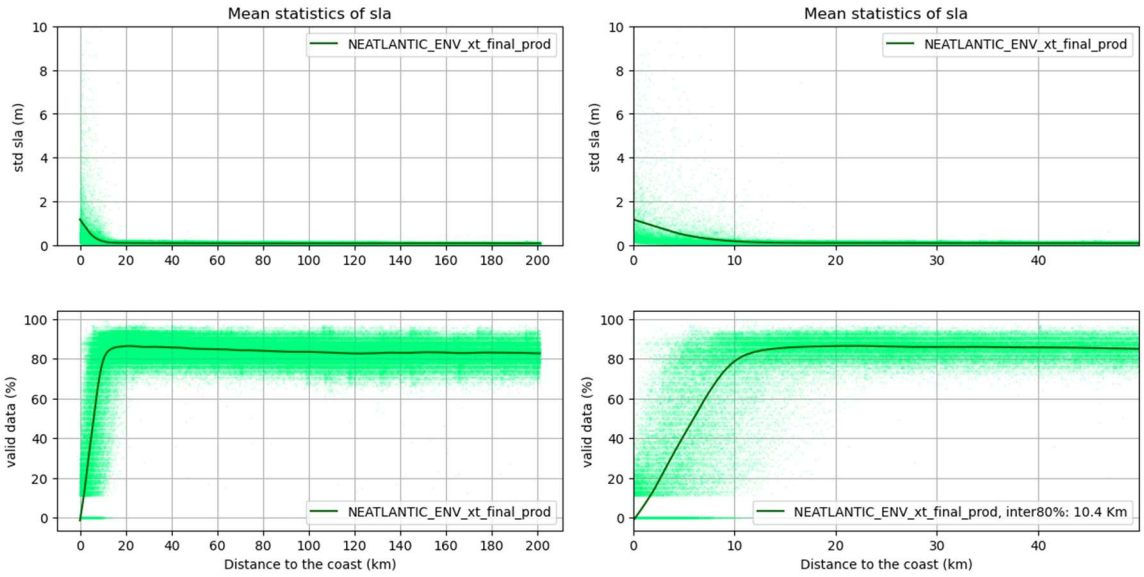

Figure 7 : Percentage of along-track valid data for SLA in the Northeast Atlantic region

3.2.3.1 Tide gauge analysis for St Jean de Luz

The St Jean de Luz tide gauge is found on the "internal angle" of the Bay of Biscay, and even though it is almost right under the nominal altimeter track, the correlation is not very good. Looking at the time series we see winter events in 2007 which are way different.

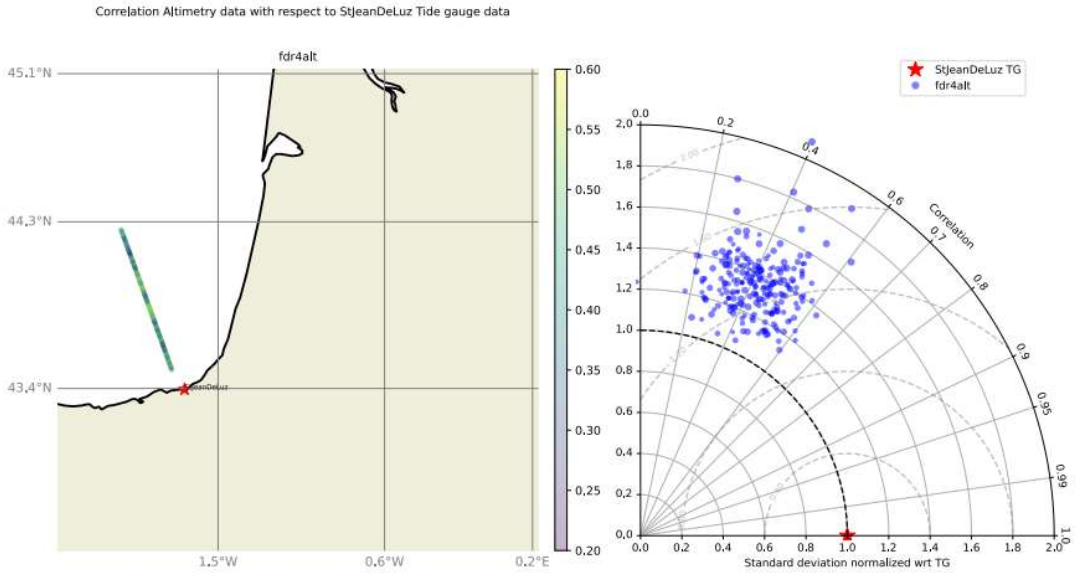

	Dist2station (km)	Dist2coast (km)	Valid data (%)	Correlation	std (m)
TG	-	-	-	-	0.053
fdr4alt	45.91	34.614	92.727	0.638	0.076

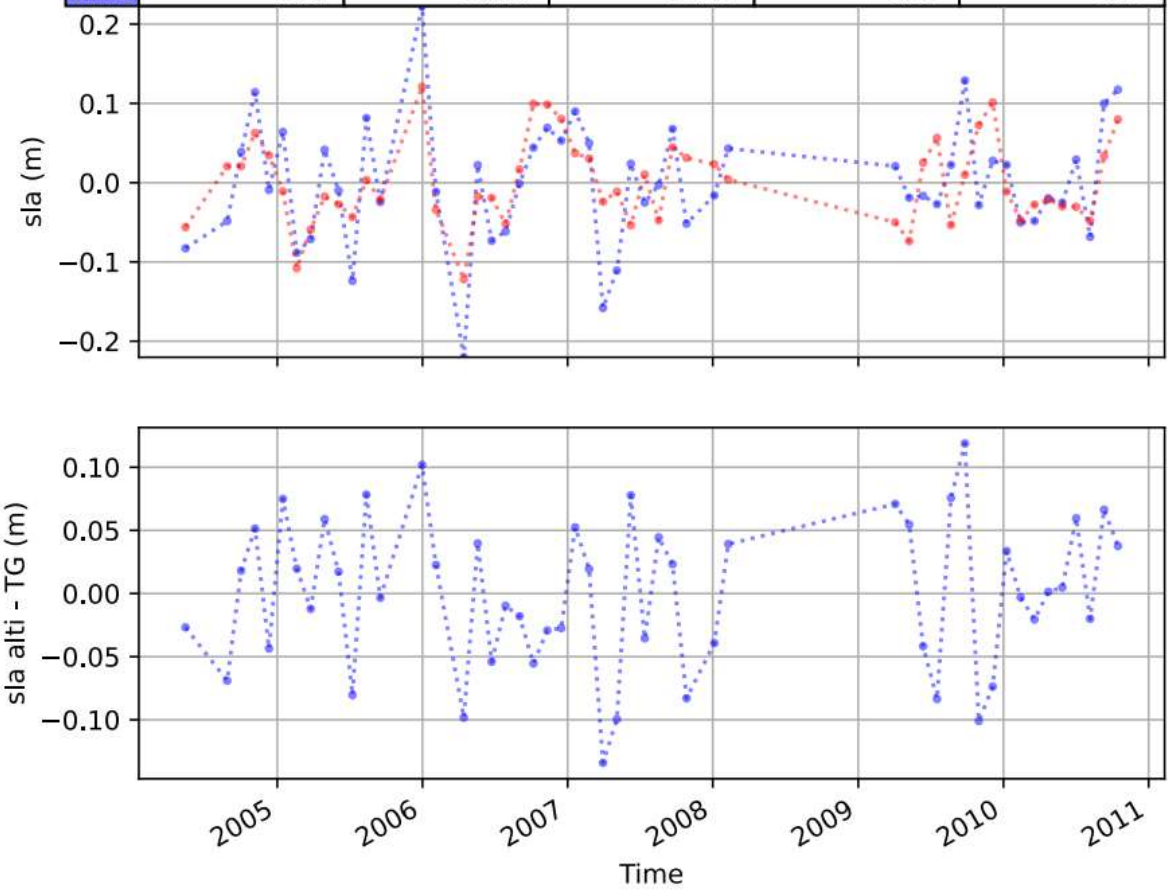

Product	Valid data (%)	Correlation	std (m)	rmsd (m)
fdr4alt	90.909	0.432	0.077	0.073

Figure 8 : Location of the St Jean de Luz tide gauge in the french Atlantic coast, with colormap of the correlation of each point (top, left). The Taylor diagram for all altimetry timeseries is plotted with respect to the tide gauge. The middle panel shows the timeseries themselves for the point with best correlation (blue) and the tide gauge (red). The bottom panel shows tabular statistics for summarizing the behaviour.

3.2.4 European Arctic

The general behaviour of this region is as expected, despite the black path on visualisation (because the region is not convex).

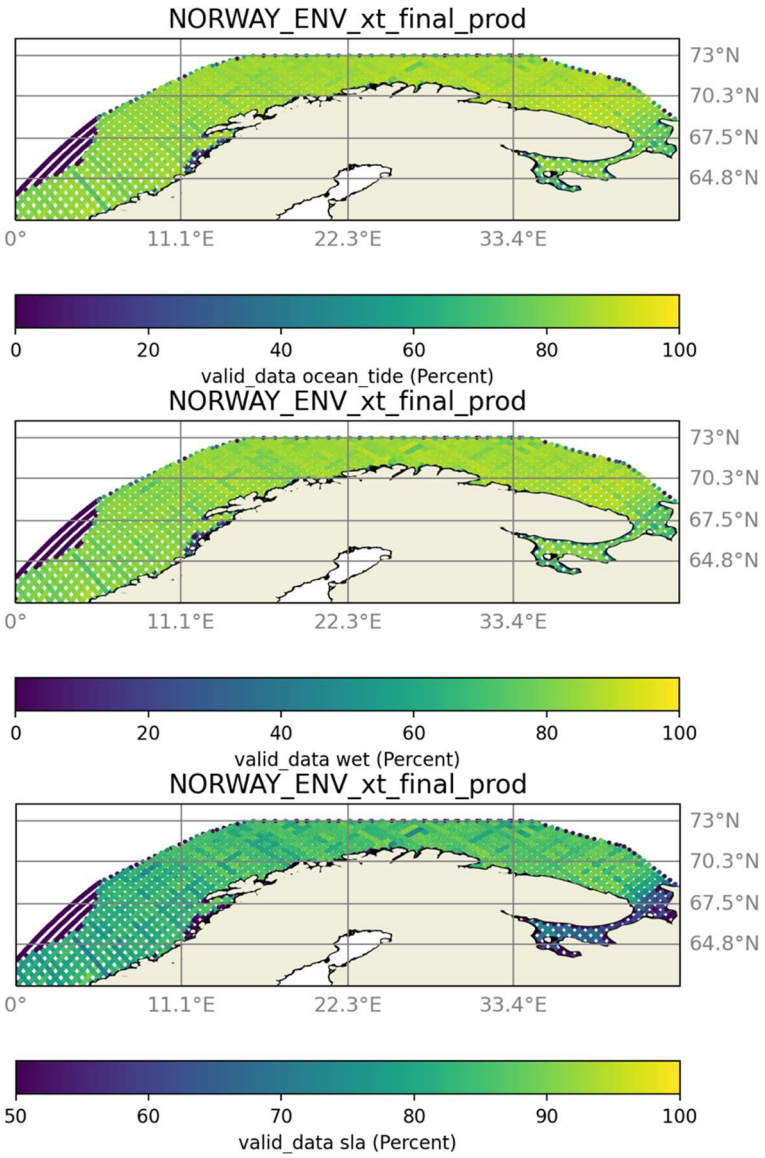

Figure 9 : Percentage of valid data in the European Arctic region for tide (top), WTC (middle)) and SLA (bottom)

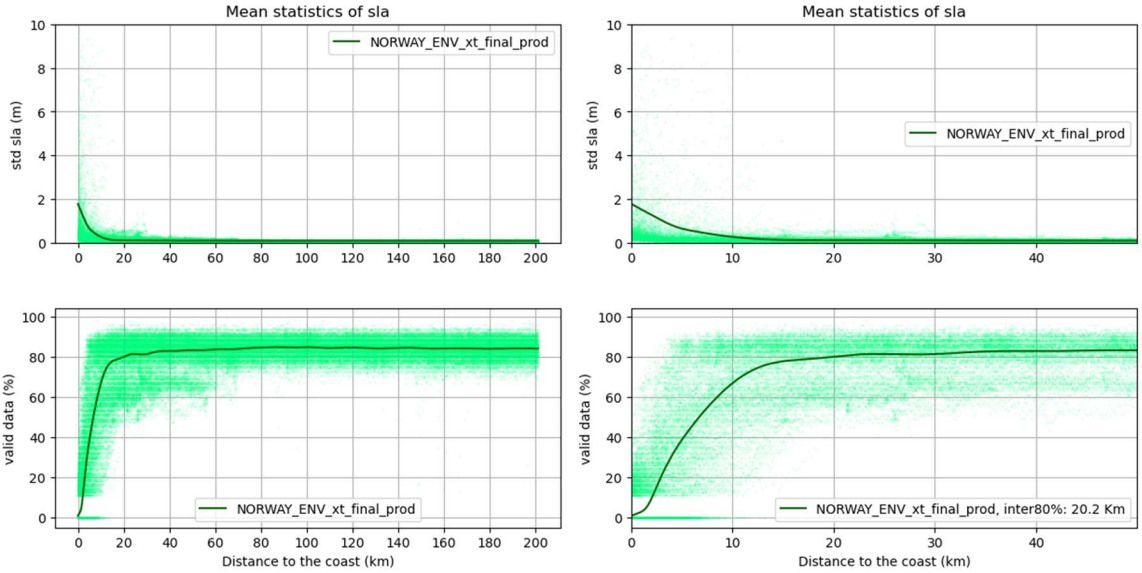

Figure 10 : Percentage of along-track valid data for SLA in the European Arctic region

3.2.5 Eastern North America

The general behaviour of this region is as expected, despite the black path on visualisation (because the region is not convex).

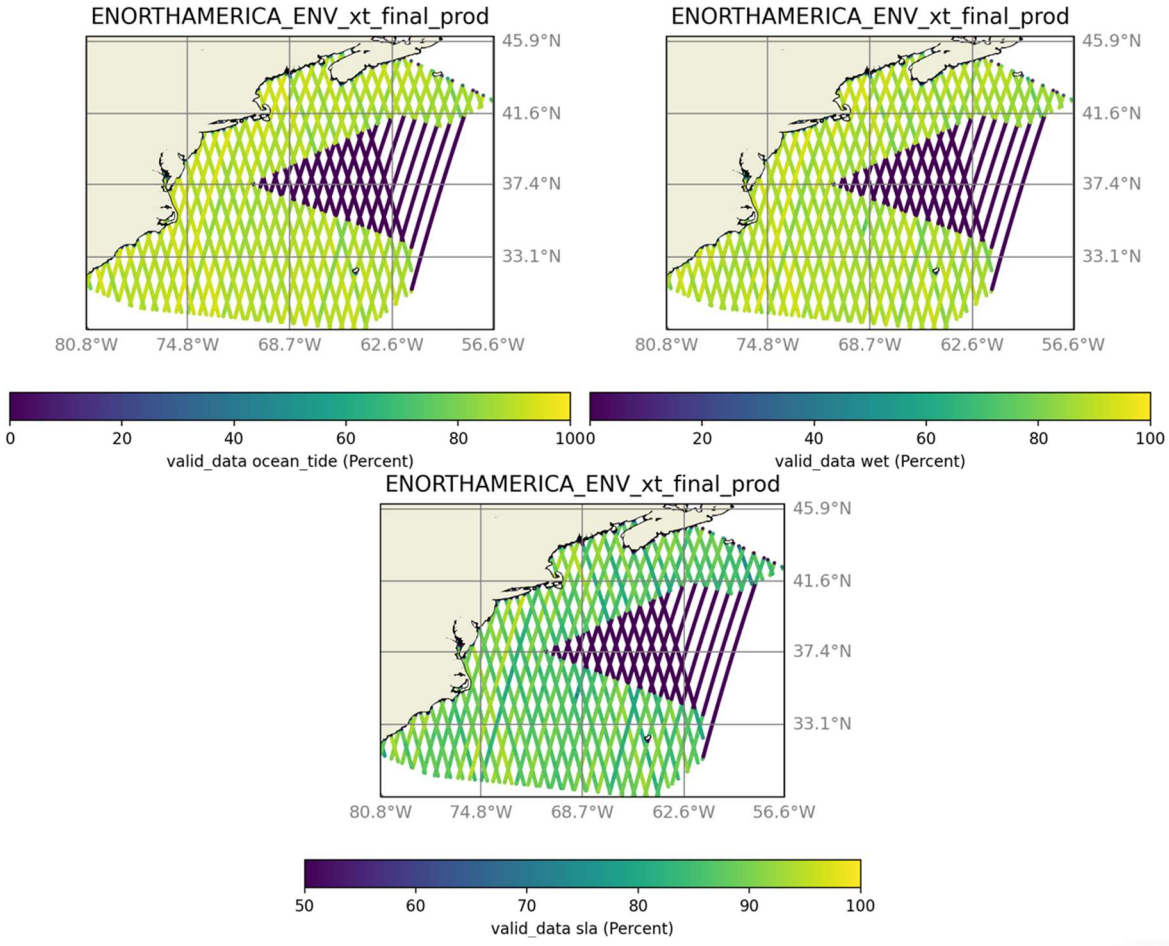

Figure – Percentage of valid data in the East North America region for tide (top left), WTC (top right) and SLA (bottom)

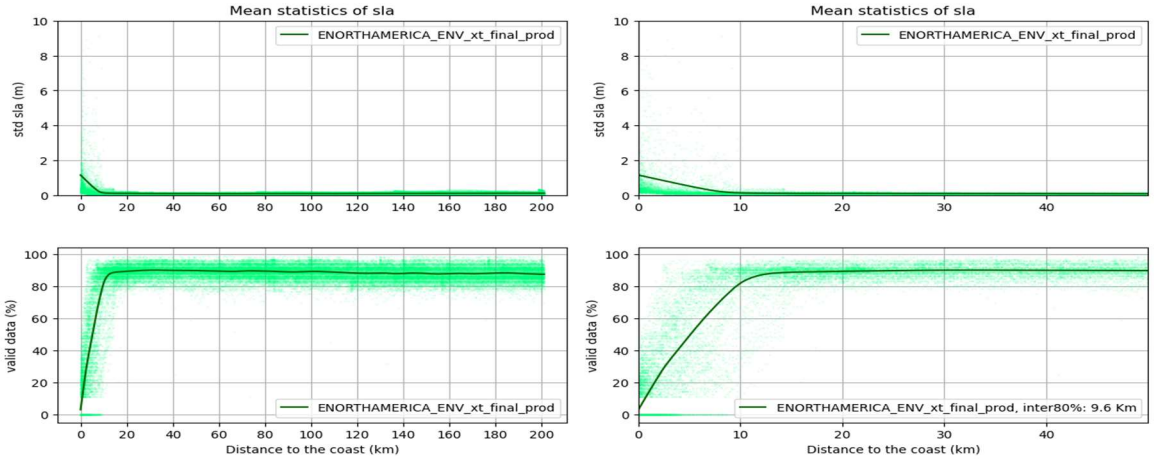

Figure 11 : Percentage of along-track valid data for SLA in the East NorthAmerica region

3.2.5.1 Tide gauge analysis for Duck

This station has very good correlation, the timeseries is very like the one from the tide gauge. Many valid data (96%) and very high correlation.

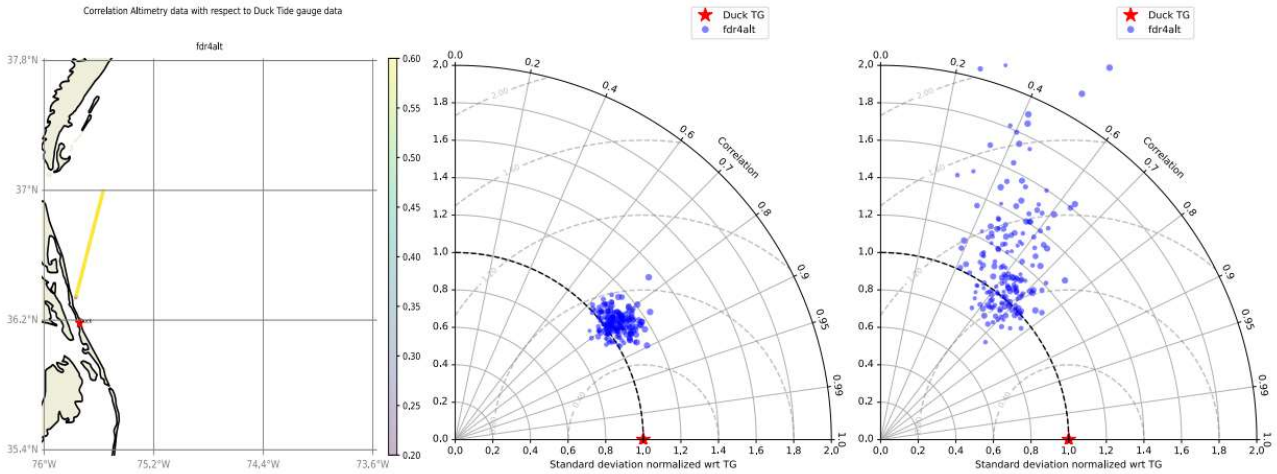

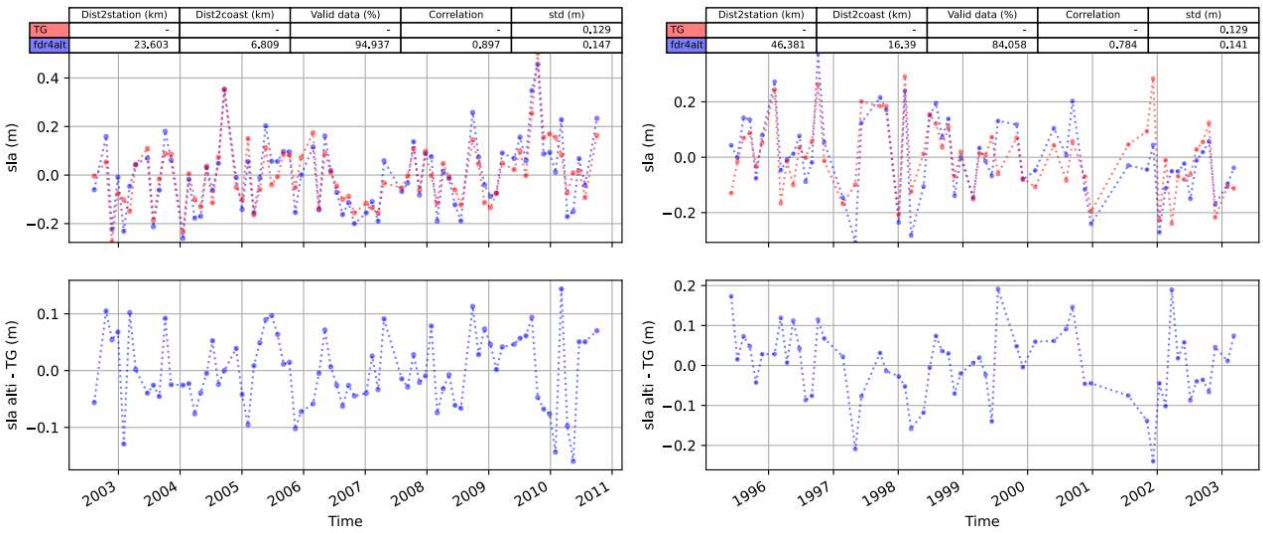

ENV ERS-2

ENV

Product	Valid data (%)	Correlation	std (m)	rmsd (m)
fdr4alt	96.065	0.801	0.138	0.086

ERS-2

Product	Valid data (%)	Correlation	std (m)	rmsd (m)
fdr4alt	84.536	0.553	0.227	0.206

Figure 12 : Location of the Duck tide gauge in the Eastern North American coast, with colormap of the correlation of each point (top, left). The Taylor diagram for all altimetry timeseries is plotted with respect to the tide gauge (for ENV top center, and ERS-2 top right). The middle panel shows the timeseries themselves for the point with best correlation (blue) and the tide gauge (red, left for ENV and right for ERS-2). The bottom panel shows tabular statistics for summarizing the behaviour for ENV and ERS-2.

3.2.5.2 Tide gauge analysis for Newport

The Newport tide gauge is very near the altimetry ground track and exhibits a high correlation of around 0.7. Very good data.

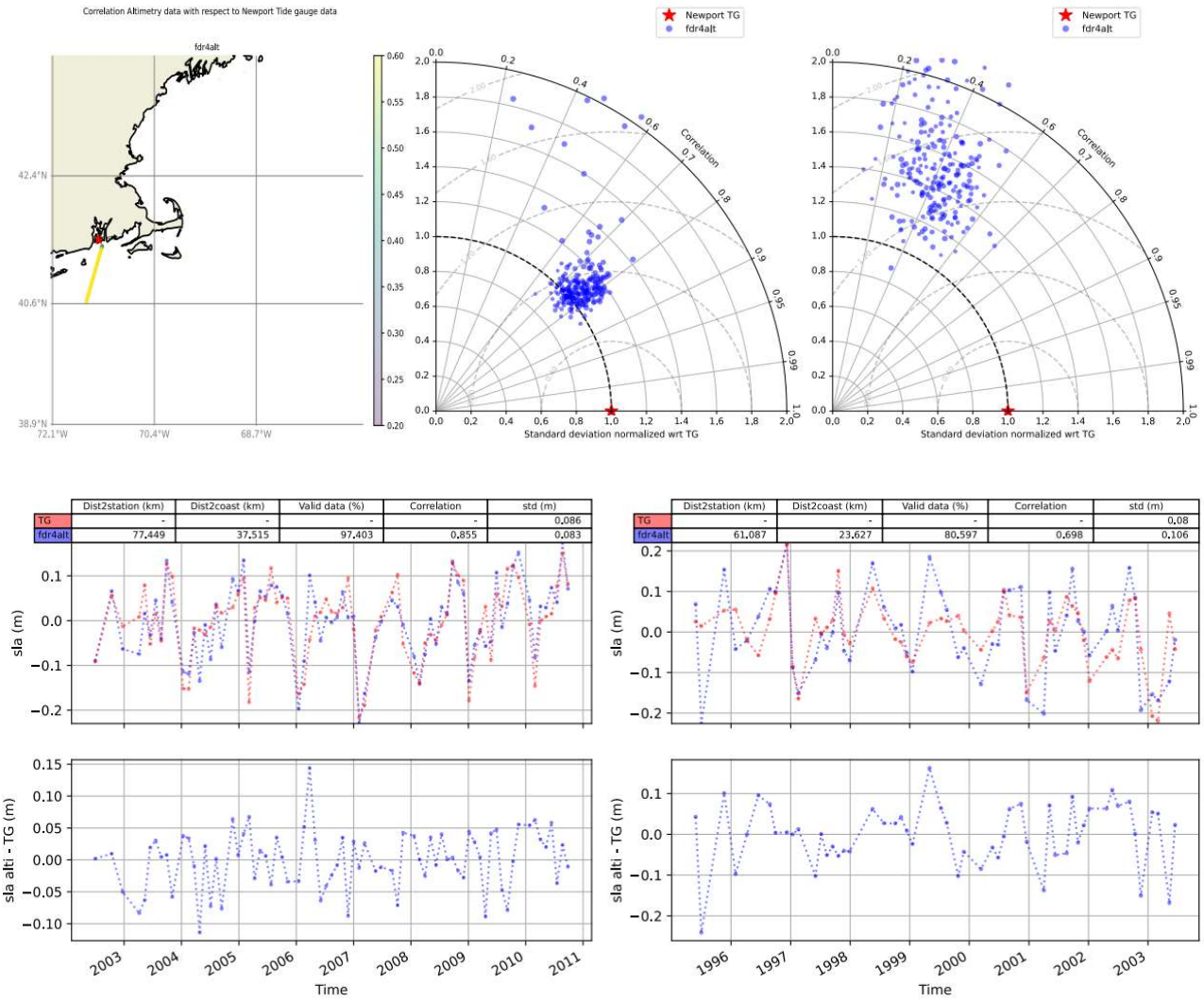

ENV ERS-2

ENV

Product	Valid data (%)	Correlation	std (m)	rmsd (m)
fdr4alt	94.56	0.736	0.096	0.068

ERS-2

Product	Valid data (%)	Correlation	std (m)	rmsd (m)
fdr4alt	85.167	0.379	0.133	0.128

Figure 13 : Location of the NewPort tide gauge in the Eastern North American coast, with colormap of the correlation of each point (top, left). The Taylor diagram for all altimetry timeseries is plotted with respect to the tide gauge (for ENV top center, and ERS-2 top right). The middle panel shows the timeseries themselves for the point with best correlation (blue) and the tide gauge (red, left for ENV and right for ERS-2). The bottom panel shows tabular statistics for summarizing the behaviour for ENV and ERS-2.

3.2.6 Eastern Australia

The general behaviour of this region is as expected, despite the black path on visualisation (because the region is not convex).

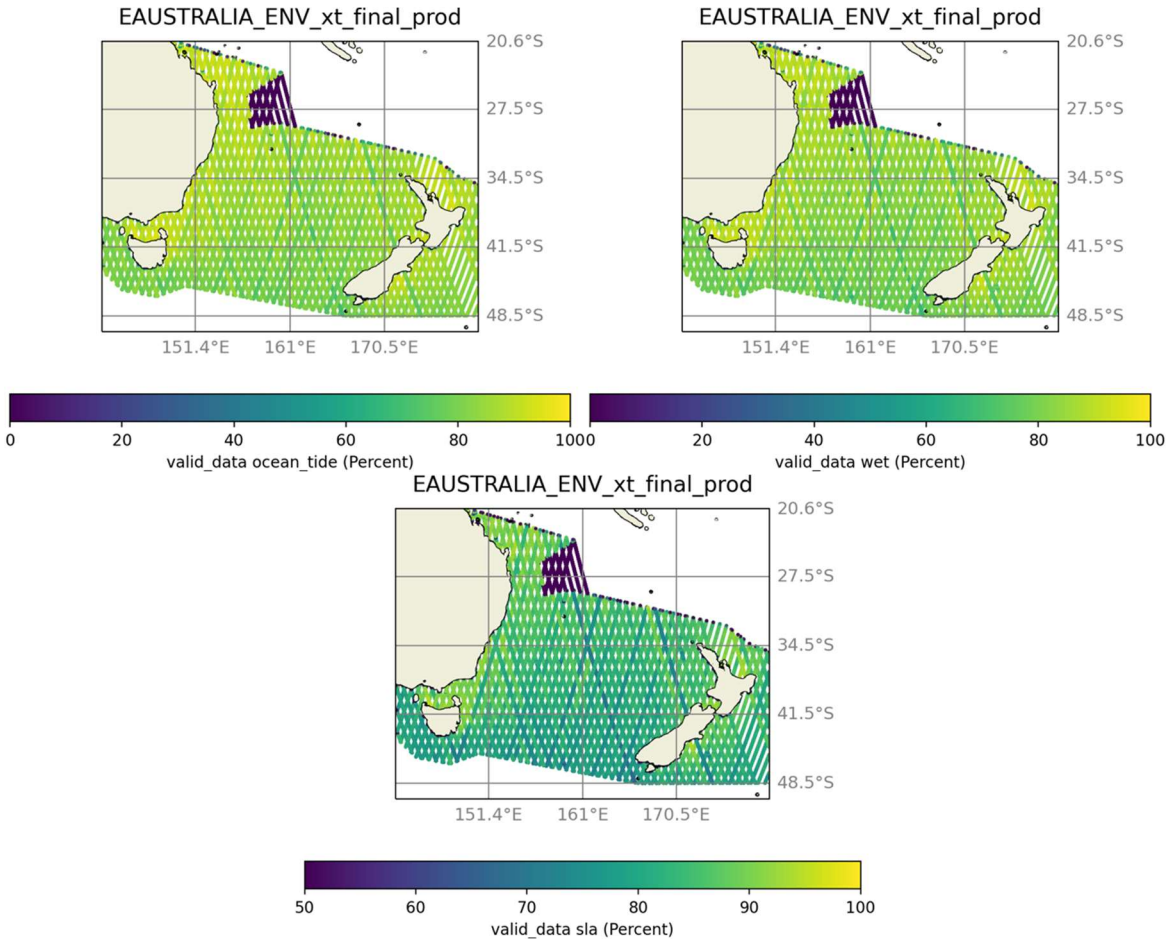

Figure 14 : Percentage of valid data in the East Australia region for tide (top left), WTC (top right) and SLA (bottom)

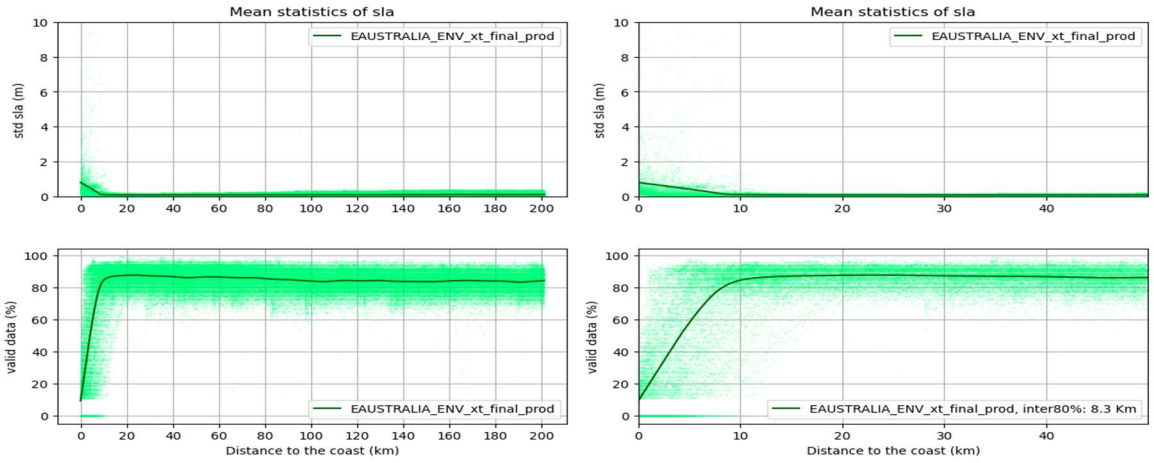

Figure 15 : Percentage of along-track valid data for SLA in the East Australia region

3.2.6.1 Tide gauge analysis for Portland

The Portland tide gauge is located on a bay, protected from direct incoming swell, but open to the ocean. The correlation is between 0.6 and 0.8 which is quite good given the distance of over 30 km to the points where the altimetric timeseries is given.

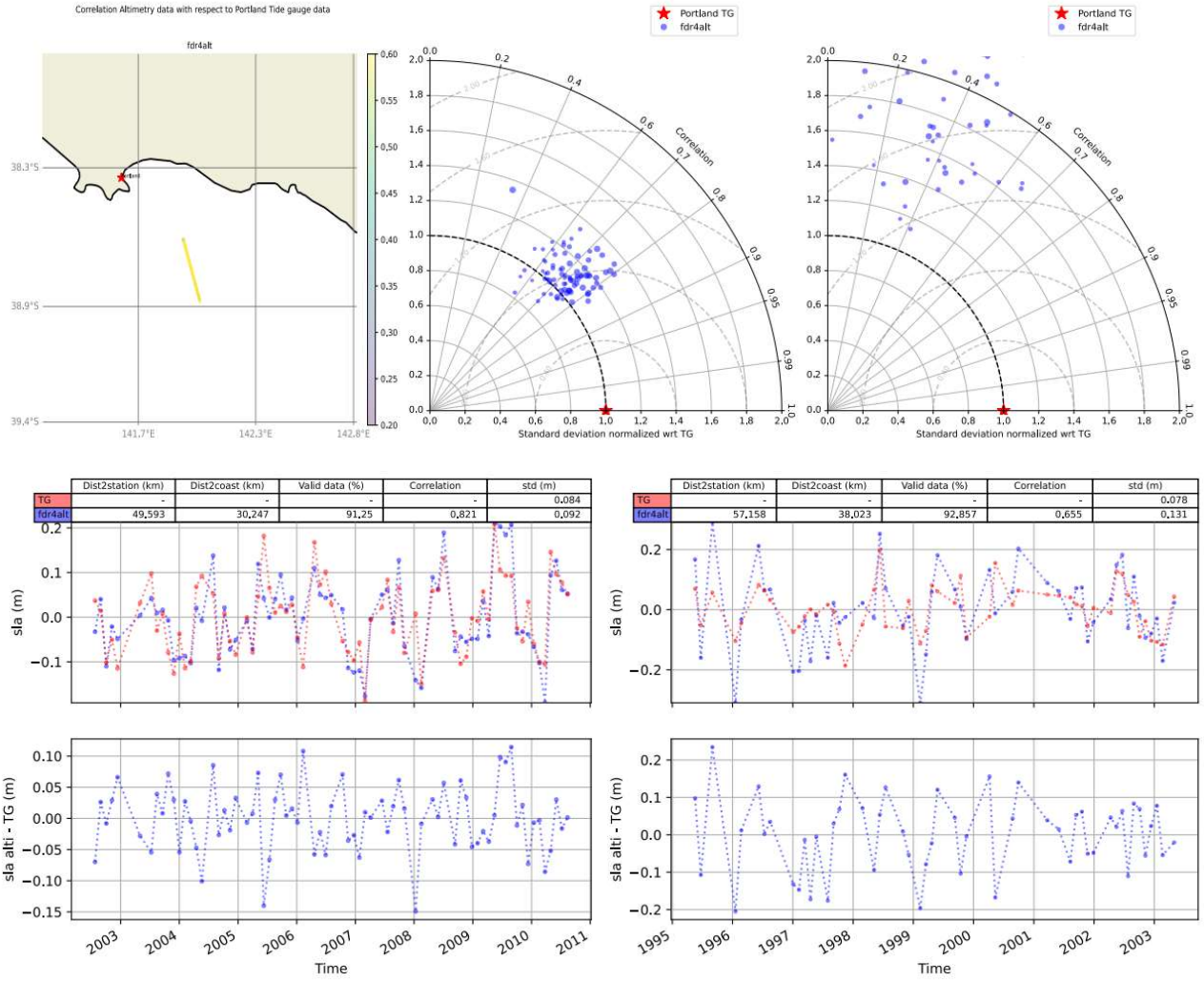

ENV ERS-2

ENV

Product	Valid data (%)	Correlation	std (m)	rmsd (m)
fdr4alt	92.681	0.701	0.099	0.073

ERS-2

Product	Valid data (%)	Correlation	std (m)	rmsd (m)
fdr4alt	83.541	0.269	0.353	0.349

Figure 16 : Location of the Portland tide gauge in the Australian coast, with colormap of the correlation of each point (top, left). The Taylor diagram for all altimetry timeseries is plotted with respect to the tide gauge (for ENV top center, and ERS-2 top right). The middle panel shows the timeseries themselves for the point with best correlation (blue) and the tide gauge (red, left for ENV and right for ERS-2). The bottom panel shows tabular statistics for summarizing the behaviour for ENV and ERS-2.

3.2.6.2 Tide gauge analysis for Wellington

This is a rather bad correlation, but the Wellington tide gauge is inside a bay without direct "view" of the altimeter track. The bay's response to sea level variations can be different, particularly if the bathymetry is such that there is nonlinear response for tides which are unaccounted for, as could be the case between two coastlines.

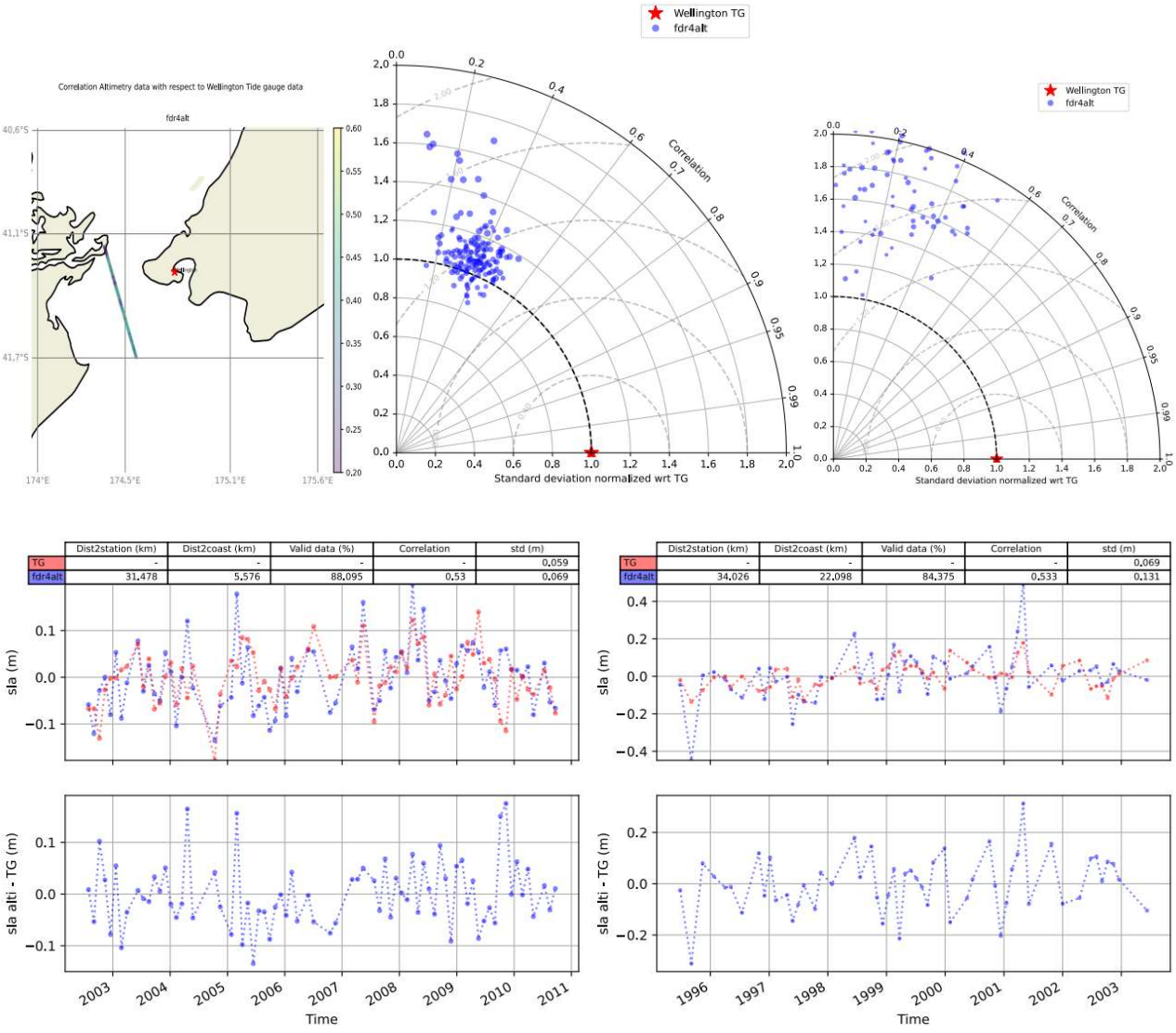

ENV *ERS-2*

ENV

Product	Valid data (%)	Correlation	std (m)	rmsd (m)
fdr4alt	91.839	0.355	0.073	0.078

ERS-2

Product	Valid data (%)	Correlation	std (m)	rmsd (m)
fdr4alt	81.007	0.188	0.18	0.183

Figure 17 : Location of the Wellington tide gauge in the Australian coast, with colormap of the correlation of each point (top, left). The Taylor diagram for all altimetry timeseries is plotted with respect to the tide gauge. The middle panel shows the timeseries themselves for the point with best correlation (blue) and the tide gauge (red). The bottom panel shows tabular statistics for summarizing the behaviour.

3.2.7 Coastal TDP validation summary and conclusions

Available data in FDR4ALT coastal data clearly follows the availability of the wet tropospheric correction. For coherency reasons, the project chose to use the WTC calculated from the FDR4ALT radiometry product, and it seems to perform well in the general case, but it is not able to fill in the missing data very near the coast. The usual strategy in coastal applications is to use the GPD+ correction (Fernandes et al. 2015) but it would need a full recalculation because of the new orbit used and the new radiometer products. This a good perspective for a FDR4ALT follow-on project. For the present project, we simply applied an editing algorithm based on the qualitative behaviour of the WTC compared to the old GPD+ WTC. It works better than no editing, but it cannot fill the gaps that GPD+ fills by using other sensor's data. The WTC for ERS-2 shows weird missing data in cycles 28 to 32.

The table below is a summary of the tide gauge data presented in this section. From this data, it is clear that ENV data is of much better quality than ERS-2, due mainly because of the quality of the Adaptive retracker used (and SSB).

It is also clear that correlations are generally very good for ENV (except for St Jean de Luz and Wellington) and much less so for ERS-2. The tide gauge analysis was not made for ERS-1 because of the very short length of continuous data, which hinders our ability to create a coherent timeseries.

Region	Tide Gauge	ENV corr	ENV rmsd	ERS-2 corr	ERS-2 rmsd
MedSea					
	Port Vendres	0,789	0,05	0,682	0,09
	Nice	0,671	0,313	*0,295*	0,112
NEA					
	St Jean de Luz	*0,432*	0,073		
NAmerica					
	Duck	0,801	0,086	0,553	0,206
	NewPort	0,736	0,068	0,379	0,128
EAustralia					
	Portland	0,701	0,073	*0,269*	0,349
	Wellington	*0,355*	0,078	*0,188*	0,183

The continuity of the solution between the ocean TDP and the coastal TDP has been checked and found very few problems.

3.3 Ocean TDP: ENVISAT

In order to clarify the improvement sources, four datasets of Sea Level Anomaly and their validity flags have been computed. Those datasets have been computed and validated at both 1Hz and 20Hz resolutions.

The first dataset referred is V3.0 of ENVISAT data (Handbook V3.0 ENVISAT) that has already been validated by calval team in 2016/2017 (ENVISAT V3.0 reprocessing CalVal report).

For a better analysis of each new component of the Sea Level Anomaly, two intermediate datasets have been used:

- The first intermediate dataset, "MLE3 with New standards" uses all new geophysical correction and new orbit. MLE3 retracking and V3.0 SSB are still used.
- The second intermediate dataset, "Adaptive" uses those new geophysical correction and new orbit with adaptive retracking and new SSB calculated by N. Tran for FDR4ALT.

In the final dataset, "Adaptive with HFA", HFA (High Frequency Adjustment) correction is added to the adaptive range. For the 1Hz dataset, SSB and HFA correction are added directly to the adaptive range and compressed from the 20Hz data set.

Particularities of 20Hz datasets:

- ✓ All geophysical corrections have been recomputed at 20Hz directly without interpolation from the 1Hz except for the wet tropospheric correction.

Particularities of the 1Hz datasets:

- ✓ Adaptive retracking fields are compressed from the 20Hz with a preliminary selection of valid retracking and bandwidth = 320Mhz (points with non-nominal bandwidth are not used during the compression step).

All standards used for each dataset are sum up in the table below. Bias referred to the bias used for the validation flag of each SLA. It corresponds of SLA mean value over a year of data (cycle 7 to 27) with a selection (Bathymetry < -1km & oceanic variability < 0.3 & coastal distance > 100km & |latitude| <66)

Table 1: Ocean TDP. Table of used standards for ENVISAT

Field	**V3.0**	**MLE3 New standards**	**Adaptive**	**Adaptive with HFA**
Orbit	Orbit POE-E	Orbit POE-F	Orbit POE-F	Orbit POE-F
Range	Range MLE3	Range MLE3	Range Adaptive + internal path delay correction	Range Adaptive + HFA correction + SSB[1] (N. Tran 2022) + internal path delay correction
SSH Interp = Orbit - Range	Sea surface height interp V3.0	Sea surface height interp MLE3	Sea surface height interp Adaptive	Sea surface height interp Adaptive with HFA
SSHA = SSH interp - geophysical corrections - MSS	Sea Surface Height anomaly V3.0	Sea Surface Height anomaly MLE3	Sea Surface Height anomaly Adaptive	Sea Surface Height anomaly Adaptive with HFA
FLAG VAL	Flag val V3.0	Flag val MLE3	Flag val Adaptive	Flag val Adaptive with HFA
Sea state bias	Non-parametric V3.0	Non-parametric V3.0	N. Tran 2022	N. Tran 2022 (included in range[1])

[1] SSB is only included on range for the 1Hz dataset

Dynamical atmospheric correction	Mog2D HR V3.0	ERA 5	ERA 5	ERA 5
Ocean Tide	FES14	FES14-B	FES14-B	FES14-B
Pole Tide	Wahr 85	Desai 2015 with MPL 2017	Desai 2015 with MPL 2017	Desai 2015 with MPL 2017
Solid Earth Tide	Cartwright-Tayler 71	Cartwright-Tayler 71	Cartwright-Tayler 71	Cartwright-Tayler 71
Dry Tropospheric correction	ECMWF GAUSS	ERA5	ERA5	ERA5
Wet Tropospheric correction	Radiometer V3.0	Radiometer with SST Gamma - FDR4ALT TDP ATM	Radiometer with SST Gamma - FDR4ALT TDP ATM	Radiometer with SST Gamma - FDR4ALT TDP ATM
Ionospheric correction	Filtered from Altimeter when Band S is available, GIM model after	GIM	GIM	GIM
Internal Tide	0	Zaron 2019 (HRET8.1)	Zaron 2019 (HRET8.1)	Zaron 2019 (HRET8.1)
Mean Sea Surface	CNES-CLS 2015	SCRIPPS combine CNES 2015/DTU 2015	SCRIPPS combine CNES 2015/DTU 2015	SCRIPPS combine CNES 2015/DTU 2015
➔ measured global bias to mss in cm (not in SSHA)	46	48	50	50

3.3.1 Data selection

Data editing is necessary to remove altimeter measurements having lower accuracy. For each dataset, a validation flag has been computed at 20Hz and at 1Hz. The validation flags computation processes have been described in the Detailed Processing Model Document (see

Document	ID	Confidentiality Level
Products Requirements & Format Specifications Document	[D-1-01] [D-2-02]	Public
Roadmap & Product Summary Document	[D-1-02]	Project Internal
Data Requirements Document	[D-1-03]	Project Internal
System Maturity Matrix	[D-1-04]	Project Internal
Examples of products	[D-1-05]	Project Internal
Review Procedure Document	[D-1-06]	Project Internal
Review Data Package	[D-1-07]	Project Internal
Phase 1 Review Report Document	[D-1-08]	Project Internal
Detailed Processing Model Document	[D-2-01]	Public
Round Robin Assessment Report Document	[D-2-03]	Public
Data Production Status Report	[D-3-01]	Project Internal
Final Output Dataset	[D-3-01]	Public
Product Validation Plan	[D-4-01]	Project Internal
Product Validation Report : FDR	[D-4-02a]	Public
Product Validation Report : Sea-Ice TDP	[D-4-02b]	Public
Product Validation Report: Land-Ice TDP	[D-4-02c]	Public

Product Validation Report : Ocean Waves TDP	[D-4-02d]	Public
Product Validation Report : Ocean & Coastal TDP	[D-4-02e]	Public
Product Validation Report: Inland Waters TDP	[D-4-02f]	Public
Product Validation Report: Atmosphere TDP	[D-4-02g]	Public
Uncertainty Characterization Definition Document	[D-5-01]	Project Internal
Uncertainty Characterization Report	[D-5-02]	Public
Product User Guide	[D-5-03]	Public
Completeness Report ALT	[D-7-01]	Public
Completeness Report MWR	[D-7-02]	Public

Table 3).

3.3.1.1 At 1Hz

As concerned the sea ice detection (first step in Detailed Processing Model Document part 2.5.3.2.1), a dedicated ice flag has been computed for each dataset, and the common land detection flag is used. The record is flagged as ice if |latitude| > 45° and if one of these criteria is met:

- |Radiometer_Wet_Tropospheric_Correction (Radiometer V3.0, Radiometer with SST Gamma - FDR4ALT TDP ATM) – ECWMF_GAUSS_Wet_Tropospheric_Correction | > 10cm
- Range_number (MLE3, Adaptive, Adaptive + HFA correction) < 17
- Peakiness > 2

After the removal of land and ice measurements, the same editing thresholds are applied to the four datasets. Statistics over data validity are computed on ocean data only, after the remove of ice measurements and selection over 0 value of surface flag GSHHG (without the Caspian Sea).

As a result, slightly more data (env. 0.8%) are valid for the final FDR4ALT dataset than for V3.0 in average (Figure 18). The right part of the figure highlights red areas where there can be around 5% more data rejected with the latest version of ENVISAT SLA. This is due to the greater dependency of standard deviation of adaptive range (from 20Hz to 1Hz compression) to high swh values (Figure 19: Ocean TDP. range rms in 1Hz measurements in function of swh estimations for MLE3 vs Adaptive retracker outputs).

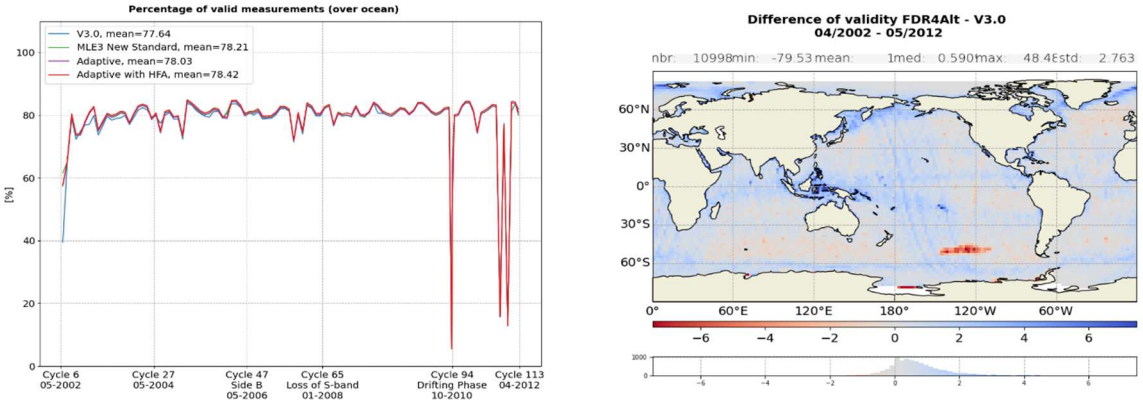

Figure 18: Ocean TDP. Percentage of valid measurements per cycle at 1Hz [left] and map of differences of validity between FDR4ALT dataset and V3.0 dataset [right].

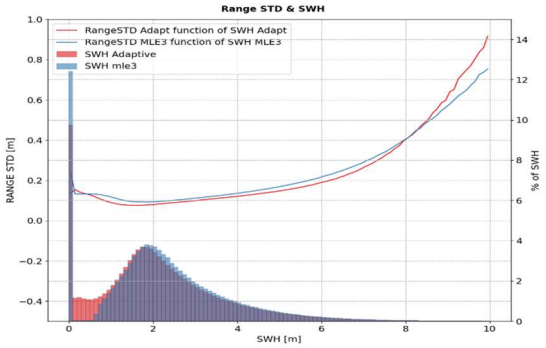

Figure 19: Ocean TDP. range rms in 1Hz measurements in function of swh estimations for MLE3 vs Adaptive retracker outputs

3.3.1.2 At 20Hz

As for the 1Hz, statistics over data validity are computed on ocean data only (after the removal of ice measurements and selection over 0 value of surface flag GSHHG (without the Caspian Sea)). The difference in valid measurements is cycle/events dependent.

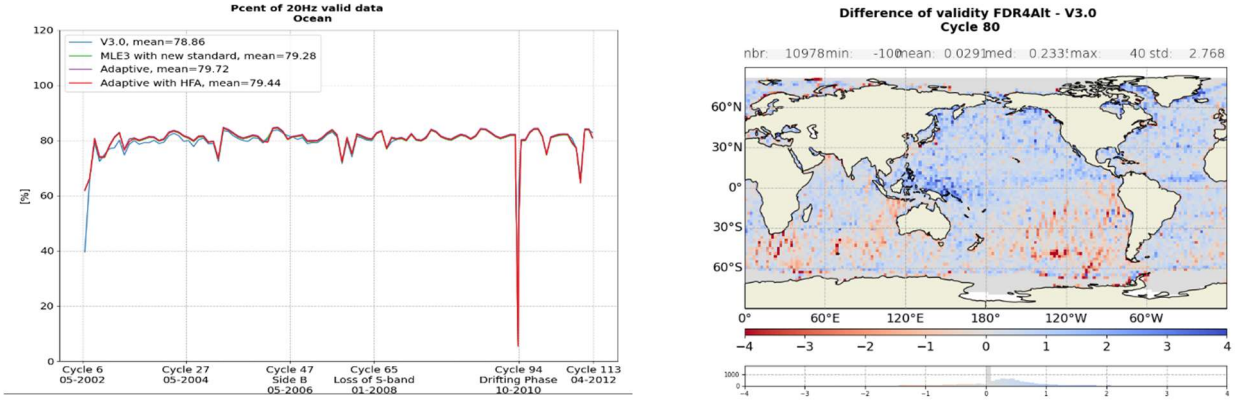

Figure 20: Ocean TDP. Percentage of 20 Hz valid measurement per cycle [left] and map of differences of validity between FDR4ALT dataset and V3.0 dataset over one cycle [right].

3.3.2 Along-track performances

3.3.2.1 At 1Hz

Note that all results presented below are calculated on valid data only and without the Caspian Sea due to its high impact on SLA variability.

To assess along-track performance, standard deviation of sea level anomaly has been computed for each dataset. The first evolution step, from v3.0 (blue curve) to MLE3 with geophysical updates (green curve) analysis leads to a better performance for v3.0 until cycle 64, then new standards reduced the standard deviation of SLA starting cycle 65. This is directly due to the ionospheric correction that has been used to calculate the SLA. No dual frequency has been computed from Adaptive retracker outputs in the frame of this project, so that GIM solution is used over the whole mission. Before cycle 65 and the loss of S-band, the use of GIM ionospheric correction model instead of the one from the altimeter increases the SLA standard deviation for all three new datasets compared to V3.0. But even before cycle 65, Adaptive retracking reduces

the standard deviation below the V3.0 level with the altimeter ionospheric correction. The global reduction of standard deviation of SLA between FDR4ALT dataset and V3.0 is monitored on figure bellow Figure 21.

Finally, the new solution leads to a reduction of the along-track standard deviation over global ocean indicator from 9.97cm to 9.93cm over the period before loss of S-band, and from 10.23cm to 9.96cm from cycle 065 to the end of the mission.

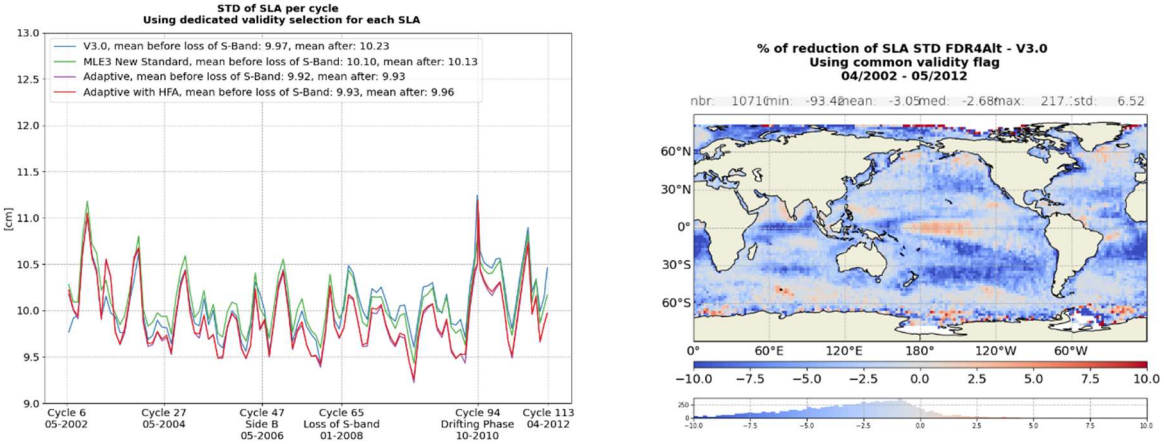

Figure 21: Ocean TDP. STD per cycle of valid SLA [left] and map of STD differences between FDR4ALT dataset and V3.0 dataset [right]

3.3.2.2 At 20Hz

The reduction of standard deviation of SLA is higher for the 20Hz dataset. Adaptive retracking and HFA correction have an important impact on the along track performance. Left part of Figure 22 shows that the reduction is global.

20Hz SLA noise has been reduced by 19%

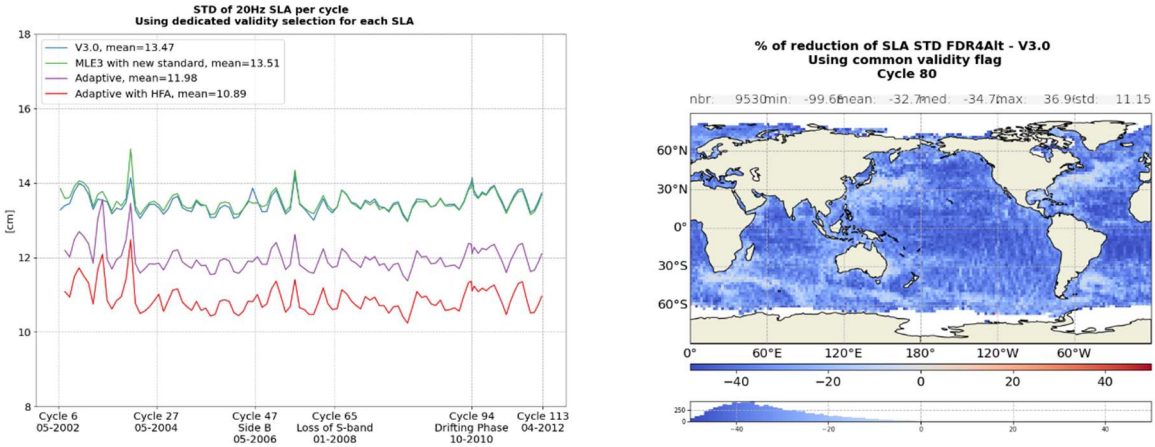

Figure 22: Ocean TDP. STD per cycle of 20Hz valid SLA [left] and map of STD differences between FDR4ALT dataset and V3.0 dataset [right]

3.3.3 Performance at mesoscales (crossovers)

10 days crossovers have been calculated for each dataset. Error at crossover is calculated with the assumption that error is equally coming from the ascending and the descending pass (standard_deviation divided by $\sqrt{2}$. First adding the new geophysical corrections, and then using the Adaptive retracker outputs both lead to a significant improvement.

The average reduction of error deduced from crossover analysis is ≃6%.

Map on the right of Figure 23 shows that this reduction is global without geographical pattern.

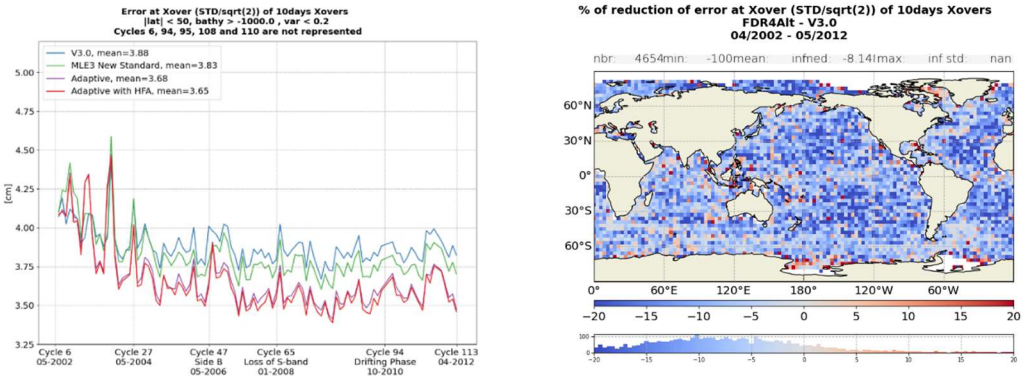

Figure 23: Ocean TDP. Error at 10days crossover per cycle [left], map of reduction of error [right]

3.3.4 Spectra, and noise analysis

Spectra have been calculated on the four datasets for the whole SLA (right part of Figure 24) and for Orbit - Range – MSS (left part of Figure 24). Differences between V3.0 and the dataset with MLE3 retracking and new standards are not significant. With spectra of (orbit - range - MSS) that does not include SSB, the adaptive retracking reduce by around 14% the noise and the HFA correction reduce by 45% the remaining noise. On the whole SLA spectra, the new 3D SSB is included with both adaptive datasets. This new SSB and adaptive retracking reduce the noise by around 26%.

Global noise reduction with adaptive retracking, 3D SSB and HFA correction is around 56%.

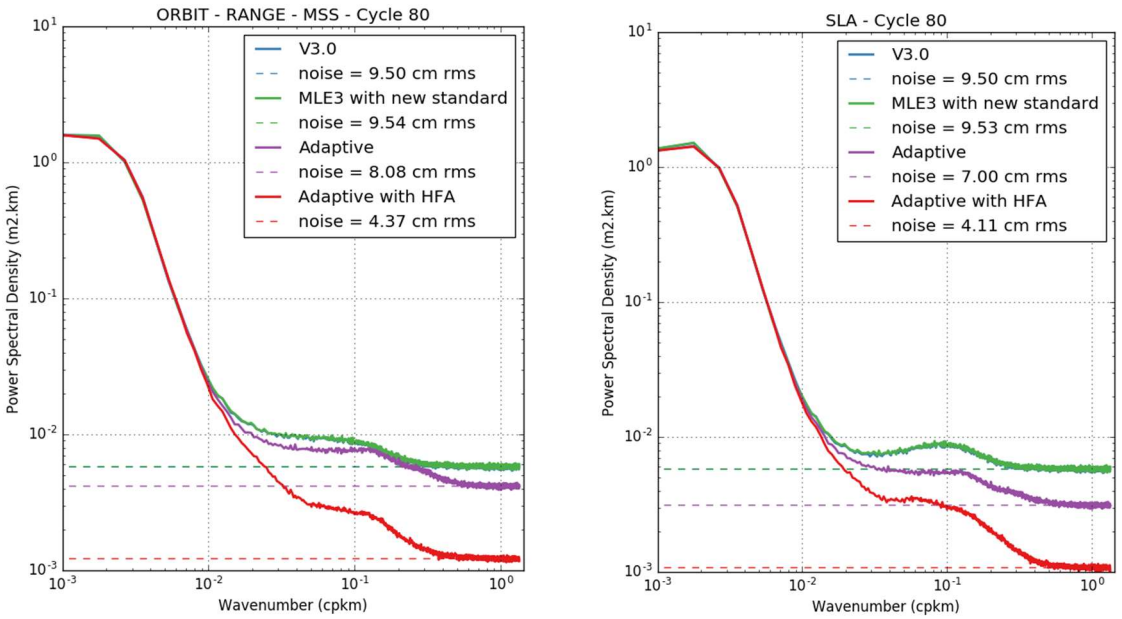

Figure 24: Ocean TDP. (orbit - range - MSS) [left] and SLA [right] spectra

3.3.5 Global Mean Sea Level trend estimation

Two GMSL have been computed for each 1Hz dataset and compared to J1, one over the whole series (2002-2012) and one over 2004-2010 to follow recommendation for the ENVISAT GMSL (see **RD 4**).

Side B bias has been computed for each dataset and is removed before the GMSL computation.

As shown in Figure 25, for the recommended period, FDR4ALT final dataset's trend (2.12mm/year) is closer to Jason-1's (2.68 mm/year) than V3.0 (3.61 mm/year). Difference with Jason's 1 has been reduced by 40%.

Trend of the differences between J1 and ENVISAT is -0.53 mm/year with FDR4ALT final dataset whereas it is 1.39mm/year with V3.0. This trend has been reduced by 61%.

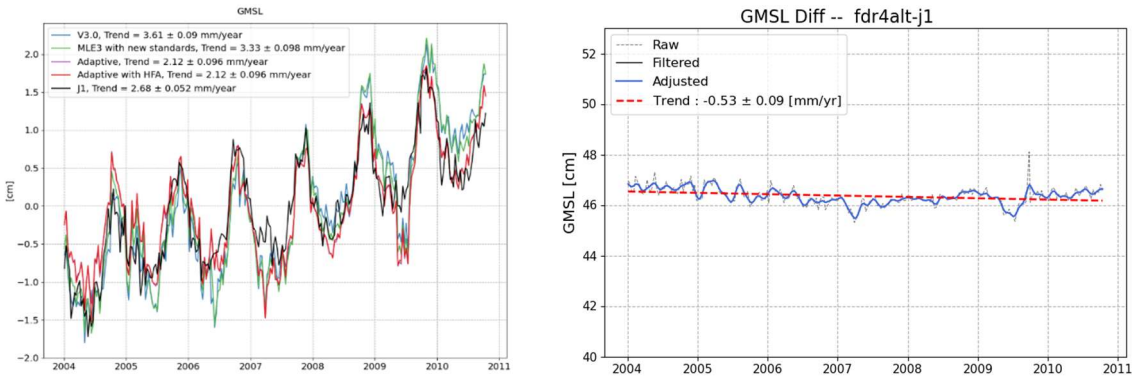

Figure 25: Ocean TDP. GMSL over the whole series and over the recommended time selection, and trend difference with Jason-1's, from 2004 onwards

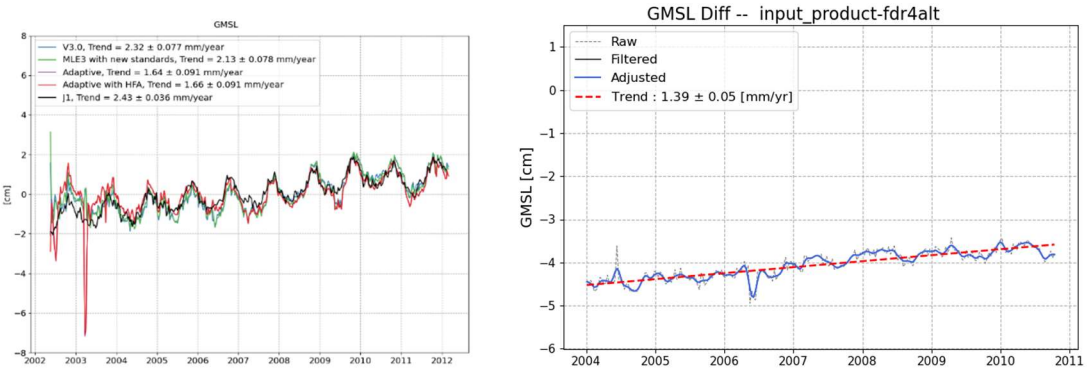

Figure 26: Ocean TDP. GMSL over the whole series and over the recommended time selection, and trend difference with Jason-1's, over the whole mission

3.3.6 Focus on wet tropospheric correction

There are globally more valid data with the FDR4ALT version of WTC over ocean (2,78% of WTC out of thresholds on FDR4ALT solution versus 4,37% with v3.0 version). But some data gaps over ocean (wtc values are set to DV in FDR4ALT solution). This could be improved during the 7Hz to 1Hz compression step.

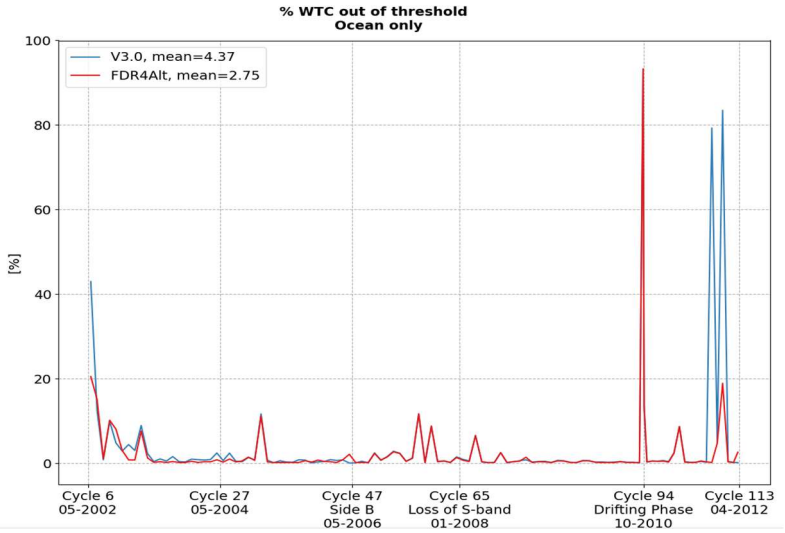

Figure 27: Ocean TDP. Cyclic monitoring of rejected points over ocean due to Wet Tropospheric Correction over ENVISAT at 1Hz

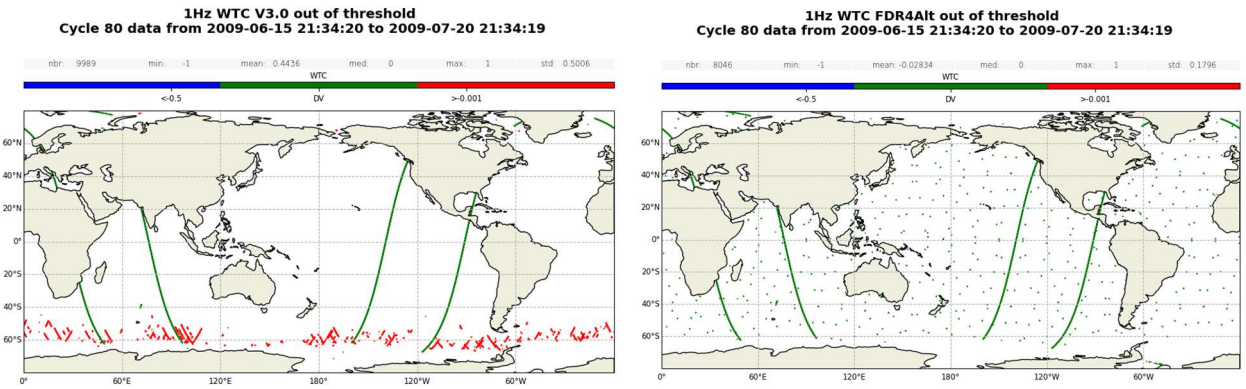

Figure 28: Ocean TDP. Map of rejected points over ocean due to Wet Tropospheric Correction over ENVISAT cycle 80 at 1Hz

3.4 Ocean TDP: ERS-2 and ERS-1

As there is no new retracker output dedicated to ocean for both ERS-2 and ERS-1 missions, two datasets of Sea Level Anomaly and their validity flags have been analyzed (three in case of ERS-2). Those datasets have been computed and validated at both 1Hz and 20Hz resolutions.

The first dataset referred is REAPER (v2) data [**RD 5**]. In the FDR4ALT dataset, the orbit and mean sea surface solutions, and geophysical corrections have been updated. In case of ERS-2, for the FDR4ALT intermediate dataset, the orbit and mean sea surface solutions, and geophysical corrections have been updated. Finally, a pseudo datation bias has been estimated and applied to correct the range estimations (see part 3.4.1).

Particularities of 20Hz datasets:

- All geophysical corrections have been recomputed at 20Hz directly without interpolation from the 1Hz except for the wet tropospheric correction and sea state bias.

All standards used for each dataset are sum up in the table below. Bias referred to the bias used for the validation flag of each SLA. It corresponds of SLA mean value over a year of data with a selection (Bathymetry < -1km & oceanic variability < 0.3 & coastal distance > 100km & |latitude| <66).

Table 2: Ocean TDP. Table of used standards for ERS-1 and ERS-2

Field	Input product	FDR4ALT = MLE3 + New standards	FDR4ALT = MLE3 + New standards + datation bias correction
Orbit	REAPER	DEOS	DEOS
Range	Range MLE3	Range MLE3	Range MLE3 + c1 * orbital_altitude_rate ERS2 : c1=- 0.00066 ERS1 : c1=- 0.00088
SSH Interp = Orbit - Range	Sea surface height interp REAPER	Sea surface height interp MLE3	Sea surface height interp MLE3

SSHA = SSH interp **- geophysical corrections** **- MSS**	Sea Surface Height anomaly	Sea Surface Height anomaly	Sea Surface Height anomaly
Validity flag	Flag val "input_product"	Flag val "fdr4alt"	Flag val "fdr4alt_datbias"
Sea state bias	Non-parametric REAPER	Non-parametric REAPER	Non-parametric REAPER
Dynamical atmospheric correction	Mog2D HR REAPER	**For ERS-1** Mog2D HR REAPER until cycle 63 included T-UGO with ERA 5 pressures for cycle 64 onwards **For ERS-2** T-UGO with ERA 5 pressures	**For ERS-1** Mog2D HR REAPER until cycle 63 included T-UGO with ERA 5 pressures for cycle 64 onwards **For ERS-2** T-UGO with ERA 5 pressures
Ocean Tide	GOT4V7 (load tide and equil_lp added from REAPER product)	FES14-B (load tide and equil_lp included)	FES14-B (load tide and equil_lp included)
Pole Tide	Wahr 85	Desai 2015 with MPL 2017	Desai 2015 with MPL 2017
Solid Earth Tide	Cartwright-Tayler 71	Cartwright-Tayler 71	Cartwright-Tayler 71
Dry Tropospheric correction	ECMWF GAUSS	ERA5	ERA5
Wet Tropospheric correction	Radiometer V3.0	Radiometer with SST Gamma - FDR4ALT TDP ATM	Radiometer with SST Gamma - FDR4ALT TDP ATM
Ionospheric correction	NIC09	**For ERS-2** GIM for ERS-2 **For ERS-1** NIC09 + 0.8mm bias (NIC to GIM averaged difference) before cycle 105 included and GIM for cycle 106 onwards for ERS-1	**For ERS-2** GIM for ERS-2 **For ERS-1** NIC09 before cycle 105 included and GIM for cycle 106 onwards for ERS-1
Internal Tide	0	Zaron 2019 (HRET8.1)	Zaron 2019 (HRET8.1)
Mean Sea Surface	CNES-CLS 2001	SCRIPPS combine CNES 2015/DTU 2015	SCRIPPS combine CNES 2015/DTU 2015
➔ measured global bias to mss in cm (not in SSHA)	67	65	65

3.4.1 Pseudo datation bias

Using crossover points we can estimate the pseudo time tag bias in data by regressing the SSH differences at crossovers against the orbital altitude rate. This method will merge true time-tag errors and other errors correlated to the altitude rate, thus the "pseudo". The mean pseudo time-tag value is about -0.66ms for ERS-2 (Figure 29), with a long-term temporal variability (the time-tag seems higher at the beginning and lower at the end of the period). Given that the orbital altitude rate can reach 25 m/s, this represents a resulting SSH error of about 1 cm. In the frame of the FDRALT project, we choose to correct the whole series which a -0.66ms value from this analysis for ERS2 and 0.88ms bias for ERS1, this could be better corrected by

understanding the origin of this datation bias. The pseudo datation bias is now analysed thanks to the same method after applying this correction on ssh estimations, resulting in the red curve of Figure 29. The estimation is more centered round 0. In case of ERS2, the value is slightly negative before 2000 and positive after. Note than a peak is visible (upper than 1ms) for cycle 061 and could be further investigated. Note that in case of ERS1, due to the non-homogeneity length of cycles, from 3 days to 168 days, the computation has been done using a 10days splitting of the data.

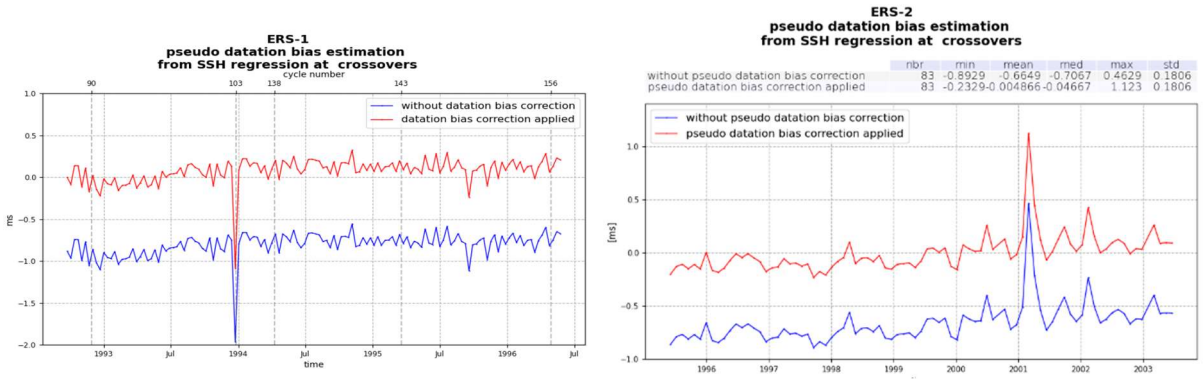

Figure 29: Ocean TDP. ERS1 (left) and ERS2 (right) pseudo datation bias

3.4.2 Duplicated points in REAPER files

During the validation process, it appears that duplicated points (points with near the same datation) are included in REAPER data at 1Hz for ERS-2 and ERS-1. It could be due to compression step anomaly during REAPER data processing. Note that these points have been removed in the FDR4ALT provided files **for ERS-1 only**. A point is removed if the distance to neighbour point is lower than 30% of the expected value. As a consequence, in case of ERS-1, the number of provided points at 1Hz in FDR4ALT dataset is lower than the REAPER dataset.

3.4.3 Data selection

Data editing is necessary to remove altimeter measurements having lower accuracy. For each dataset, a validation flag has been computed at 20Hz and at 1Hz. The validation flags computation processes have been described in the Detailed Processing Model Document (see

Document	ID	Confidentiality Level
Products Requirements & Format Specifications Document	[D-1-01] [D-2-02]	Public
Roadmap & Product Summary Document	[D-1-02]	Project Internal
Data Requirements Document	[D-1-03]	Project Internal
System Maturity Matrix	[D-1-04]	Project Internal
Examples of products	[D-1-05]	Project Internal
Review Procedure Document	[D-1-06]	Project Internal
Review Data Package	[D-1-07]	Project Internal

Phase 1 Review Report Document	[D-1-08]	Project Internal
Detailed Processing Model Document	[D-2-01]	Public
Round Robin Assessment Report Document	[D-2-03]	Public
Data Production Status Report	[D-3-01]	Project Internal
Final Output Dataset	[D-3-01]	Public
Product Validation Plan	[D-4-01]	Project Internal
Product Validation Report : FDR	[D-4-02a]	Public
Product Validation Report : Sea-Ice TDP	[D-4-02b]	Public
Product Validation Report: Land-Ice TDP	[D-4-02c]	Public
Product Validation Report : Ocean Waves TDP	[D-4-02d]	Public
Product Validation Report : Ocean & Coastal TDP	[D-4-02e]	Public
Product Validation Report: Inland Waters TDP	[D-4-02f]	Public
Product Validation Report: Atmosphere TDP	[D-4-02g]	Public
Uncertainty Characterization Definition Document	[D-5-01]	Project Internal
Uncertainty Characterization Report	[D-5-02]	Public
Product User Guide	[D-5-03]	Public
Completeness Report ALT	[D-7-01]	Public
Completeness Report MWR	[D-7-02]	Public

Table 3).

As concerned the sea ice detection (first step in Detailed Processing Model Document part 2.5.3.2.1), the available in REAPER solution is reused. After the removal of land and ice measurements, the same editing thresholds are applied to the three datasets at 1Hz. Statistics over data validity are computed on ocean data only, after the remove of ice measurements and selection over 0 value of surface flag GSHHG (adding the Caspian Sea). As a result, slightly more data (env. 0.3%) are valid for the intermediate and final FDR4ALT datasets than for REAPER dataset in average (Figure 30). The main difference is for cycle 019, for which sea level anomaly variability is significantly higher in case of REAPER product than with FDR4ALT reprocessing for passes 334 to 432. Thanks to the FDR4ALT reprocessing of radiometer wet tropospheric correction (Figure 32), data are mainly more valid with the new dataset over wet areas (in orange and red on right part of Figure 31). Results from data selection at 20Hz are quite equivalent as there is no new retracking, neither sea state bias correction applied to 20 Hz data for ERS.

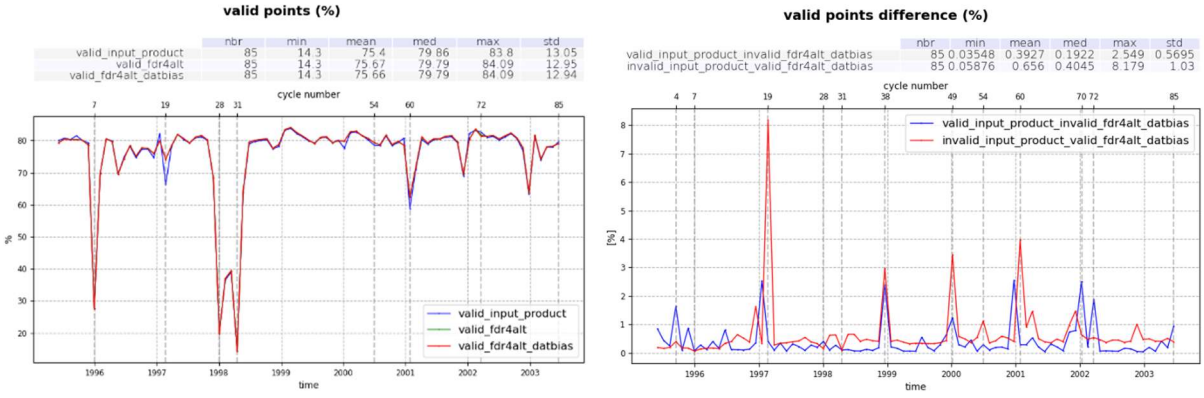

Figure 30: Ocean TDP. Percentage of ERS-2 valid measurements per cycle at 1Hz [left] and percentage of valid in one case vs invalid in the other case measurements per cycle at 1Hz [right].

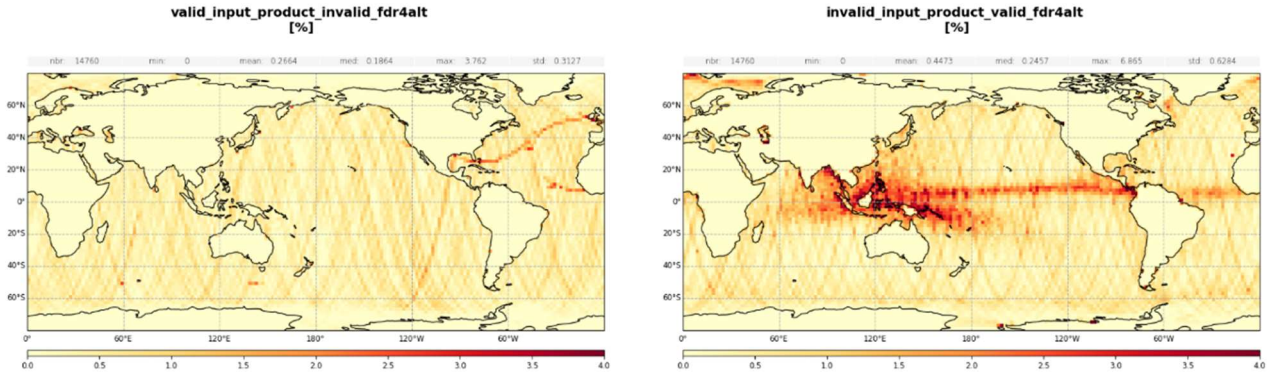

Figure 31: Ocean TDP. Map of percentage of valid in one case vs invalid in the other case measurements per cycle at 1Hz over ERS-2 cycles 1 to 85.

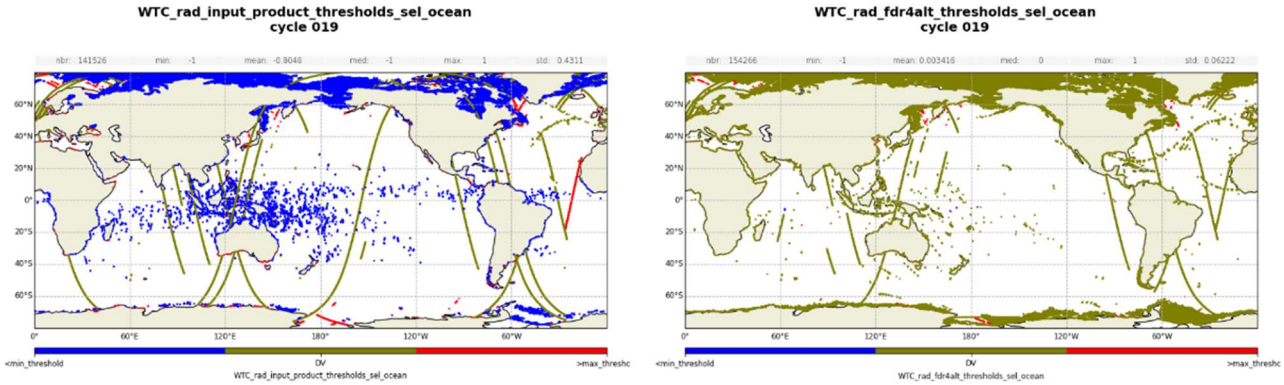

Figure 32: Ocean TDP. Map of rejected points due to wet tropospheric correction from radiometer at 1Hz over ERS-2 cycle 19, for REAPER version (left) versus FDR4ALT reprocessing version (right).

In case of ERS1, more data (env. 2.3%) are removed for the intermediate and final FDR4ALT datasets than for REAPER version in average (Figure 33).

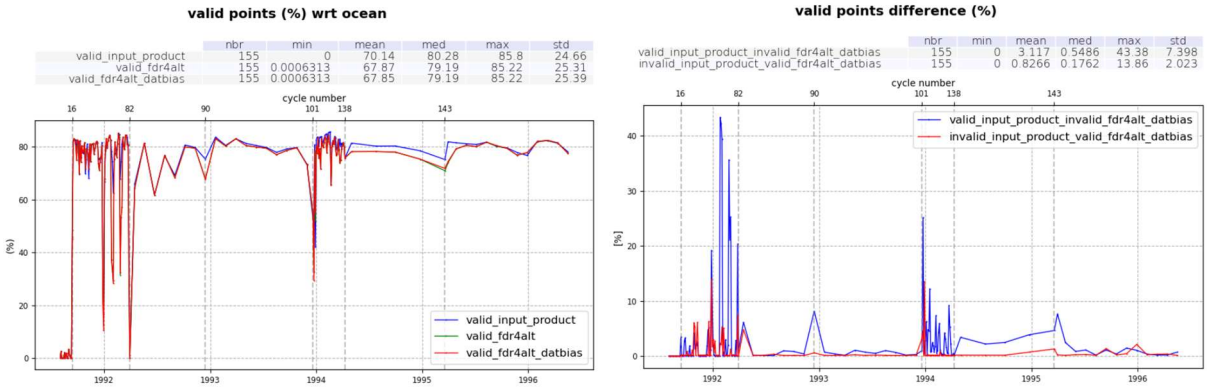

Figure 33: Ocean TDP. Percentage of ERS-1 valid measurements per cycle at 1Hz [left] and percentage of valid in one case vs invalid in the other case measurements per cycle at 1Hz [right].

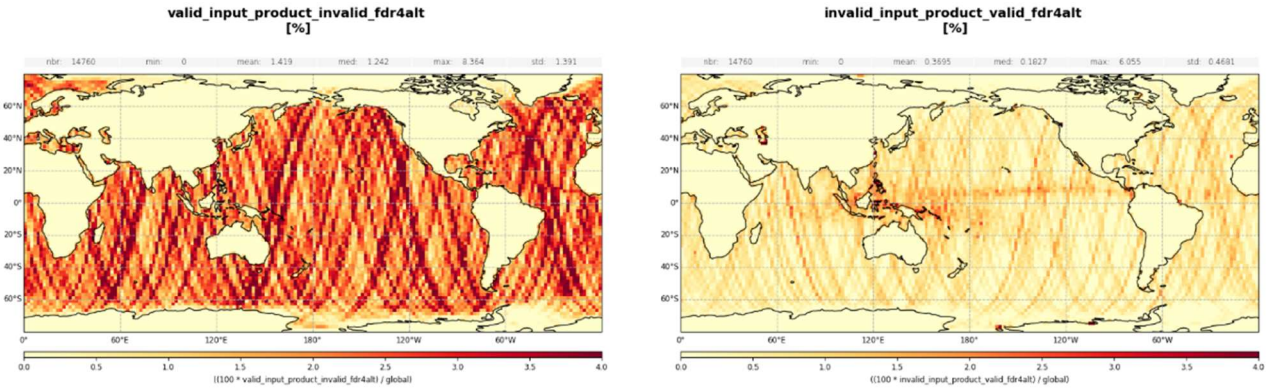

Figure 34: Ocean TDP. Map of percentage of valid in one case vs invalid in the other case measurements per cycle at 1Hz over ERS-1 cycles 2 to 156.

3.4.4 Along-track performances

Note that all results presented below are calculated on valid data only and without the Caspian Sea due to its high impact on SLA variability.

To assess along-track performance, standard deviation of sea level anomaly has been computed for each dataset. This metric is significantly reduced (by 1cm in average) with the new ERS-2 dataset over the whole mission (Figure 35), except during the *el nino* event in 1997/1998 (during such an event, along-track ssha is higher than usual in global analysis).

In case of ERS-1, standard deviation is reduced in average over the whole period, except for some cycles during the 3days cycle period at the beginning of the mission and during the drifting period between cycles 139 and 142 (Figure 37).

For both missions, in average over the whole period, regional patterns of SLA variance evolution show better results with the fdr4alt dataset (blues areas on Figure 36 for ERS-2 and Figure 38 for ERS-1).

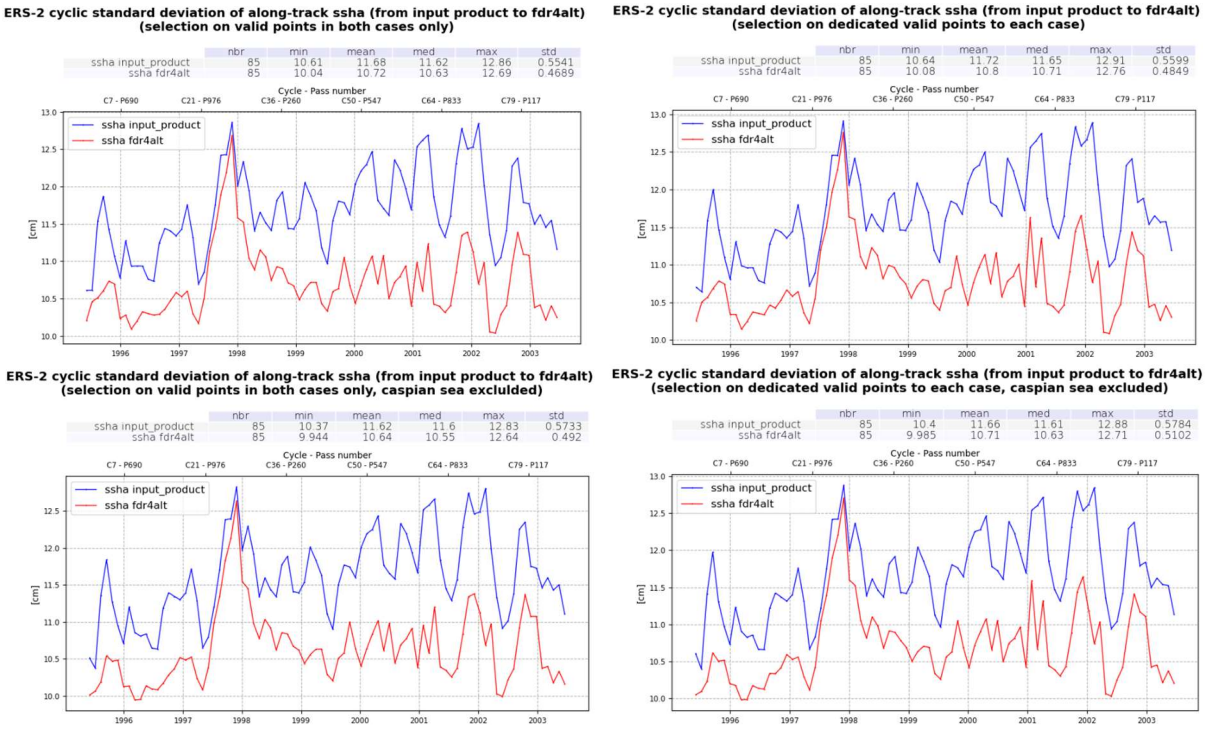

Figure 35: Ocean TDP. ERS-2 cyclic standard deviation of along-track ssha (from input product to fdr4alt), selection on valid points in both cases only (left) or considering dedicated validity status for each case (right), excluding Caspian Sea (bottom).

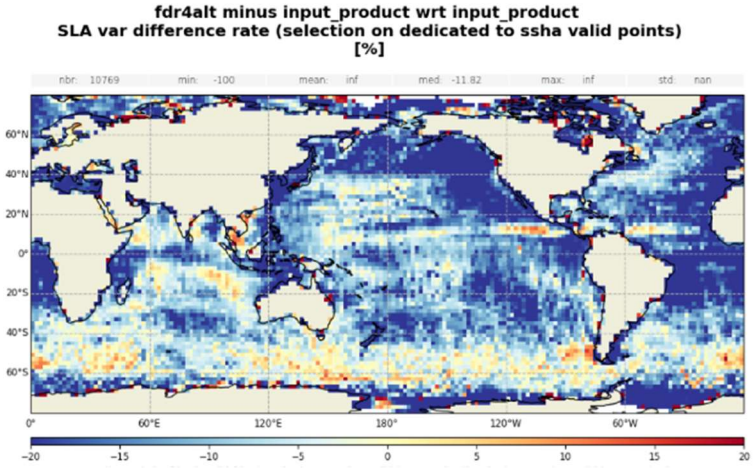

Figure 36: Ocean TDP. ERS-2 map of ssha variance reduction (in blue), thanks to fdr4alt project (from input product to fdr4alt), over the ERS-2 cycles 1 to 85, considering dedicated validity status for each case.

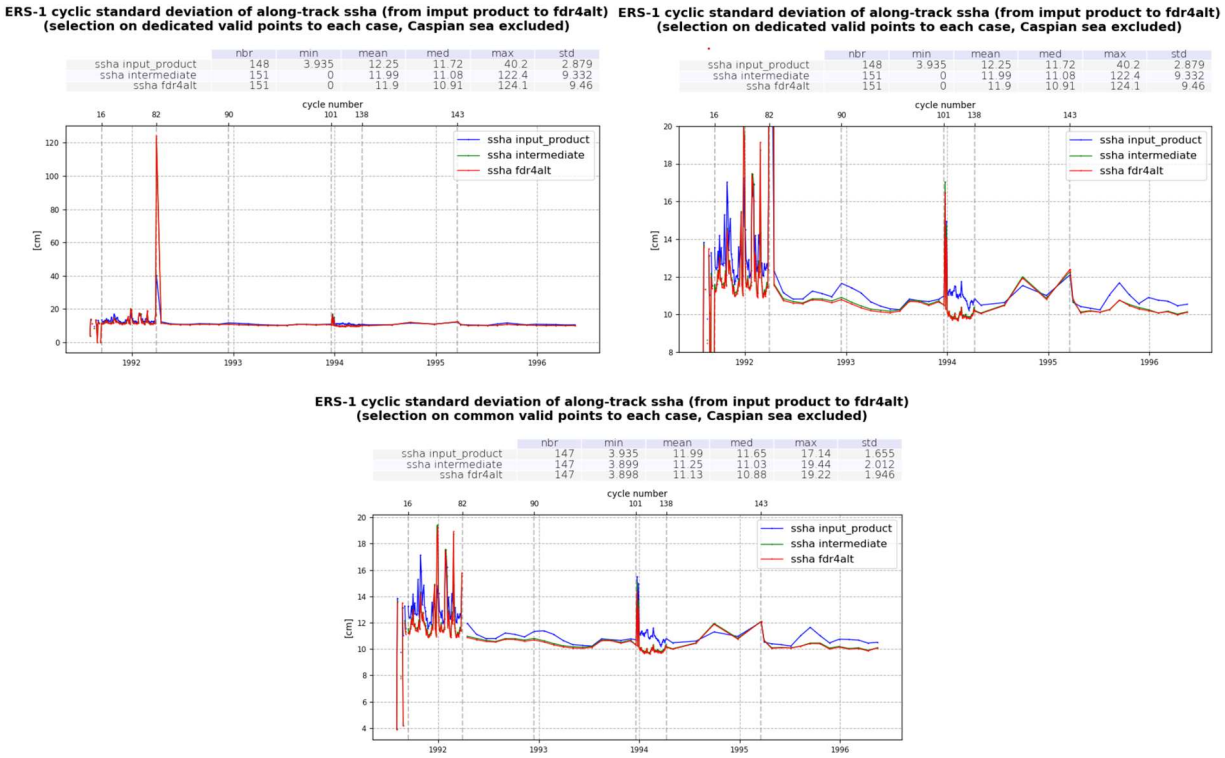

Figure 37: Ocean TDP. ERS-1 cyclic standard deviation of along-track ssha (from input product to fdr4alt), selection on valid points in both cases only (bottom) or considering dedicated validity status for each case (top, with a focus for 8 to 20cm values on the right)), excluding Caspian Sea

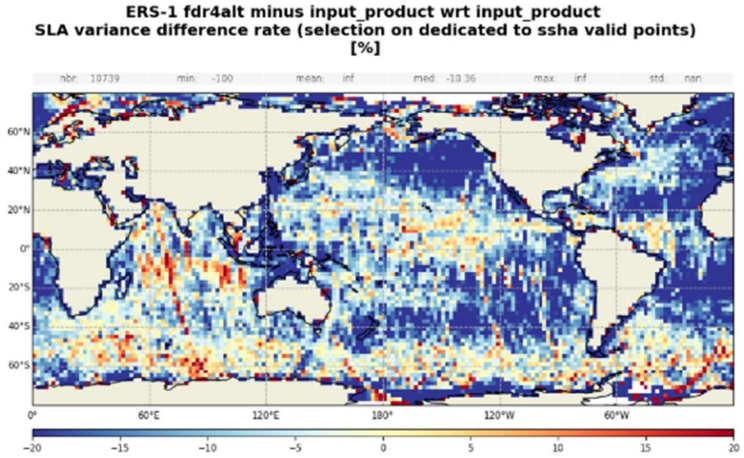

Figure 38: Ocean TDP. ERS-1 map of ssha variance reduction (in blue), thanks to fdr4alt project (from input product to fdr4alt), over the ERS-1 cycles 2 to 156, considering dedicated validity status for each case.

3.4.5 Performance at mesoscales (crossovers)

10 days crossovers have been calculated for each 1Hz dataset. Mean of SSH differences at crossovers is analyzed over 1 to 85 ERS-2 cycles. The spatial distribution of mean SSH differences at crossovers for ERS-2 estimated from REAPER and intermediate fdr4alt data (Figure 39) show a strong hemispheric pattern which points toward a remaining time-tag bias in the data. By correcting this pseudo datation bias (see also part 3.4.1), these strong hemispheric biases are significantly reduced (bottom right of Figure 39).

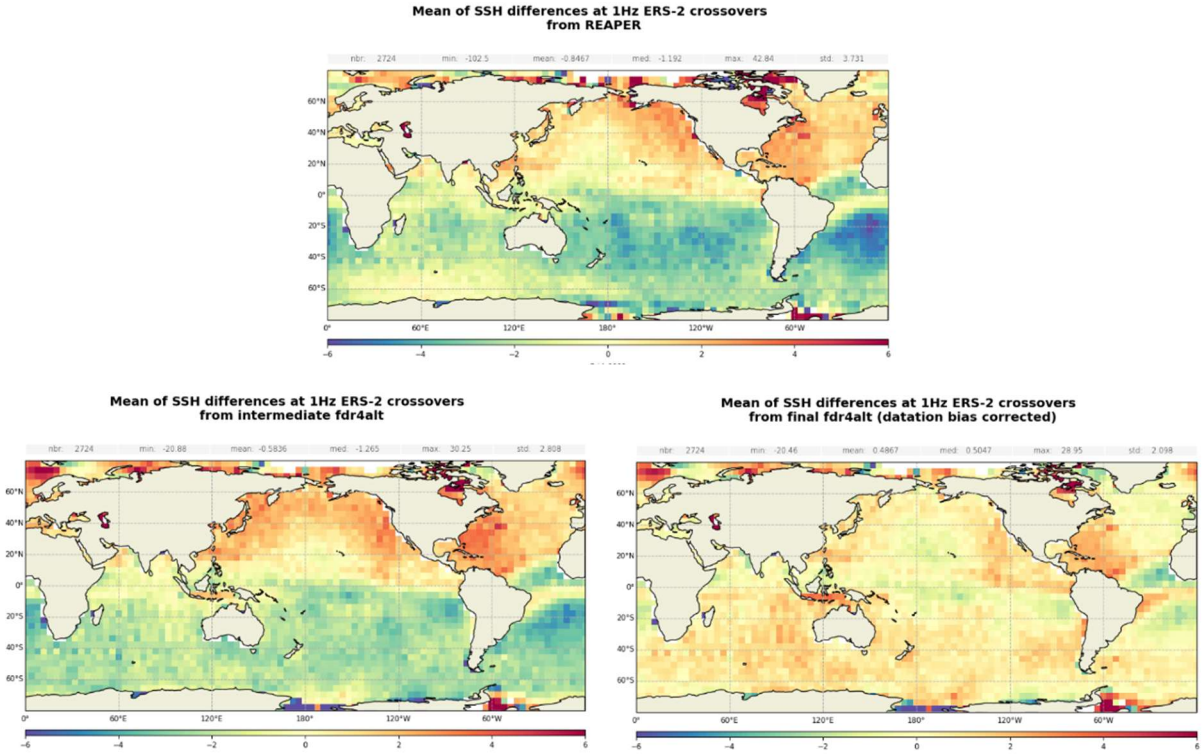

Figure 39: Ocean TDP. ERS-2. Mean of SSH differences at crossovers for REAPER (top) intermediate fdr4alt (bottom left) and final fdr4alt (bottom right) datasets.

Error at crossover is calculated with the assumption that error is equally coming from the ascending and the descending pass (standard deviation divided by $\sqrt{2}$. First adding the new geophysical corrections, and then using the datation bias correction both lead to a significant improvement, from REAPER to intermediate solution, the variance reduction is 4.6cm², and including the datation bias correction leads to a total reduction of 7.5cm² (Figure 40). Map on Figure 41 shows some geographical patterns with a higher reduction level.

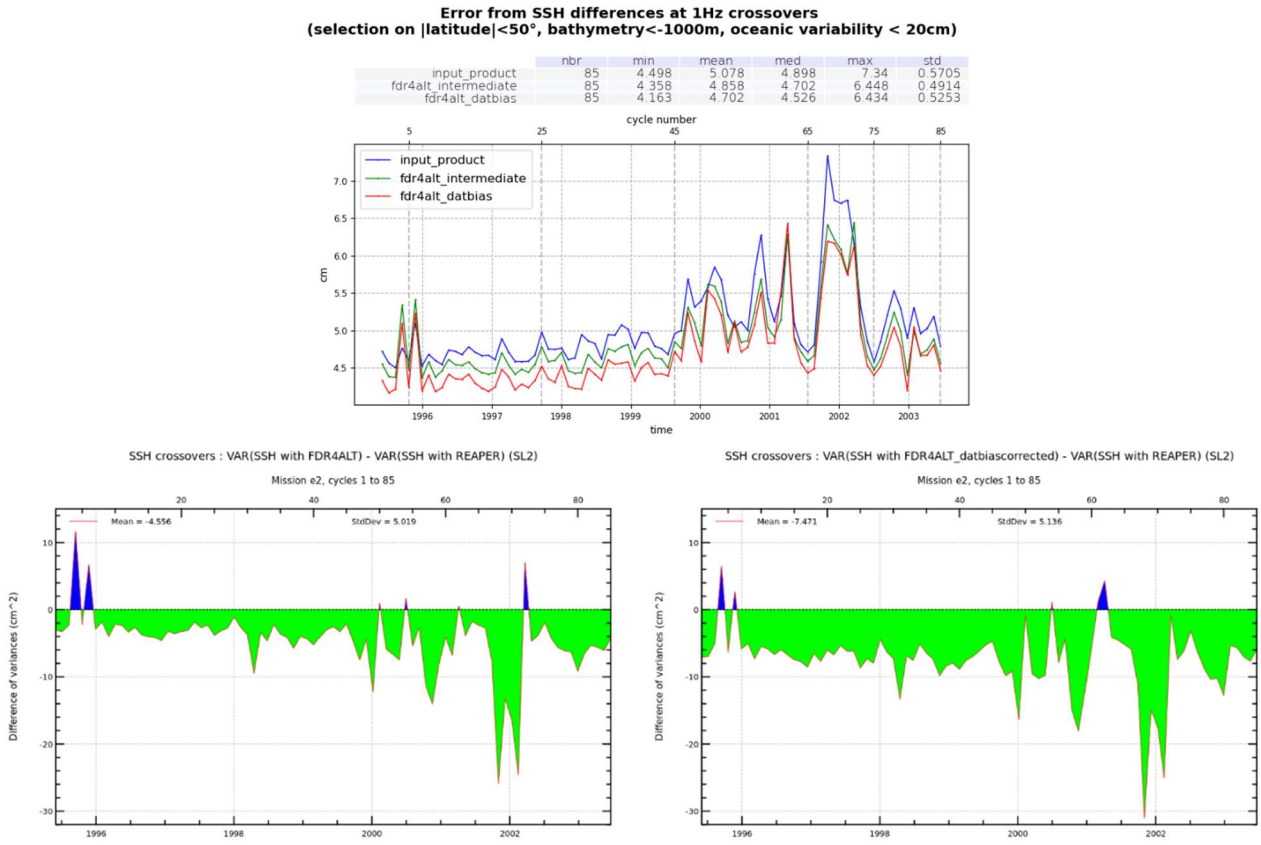

Figure 40: Ocean TDP. Cyclic monitoring of error (top) and variance reduction (bottom) at crossovers (1hz dataset) for ERS-2, from REAPER to intermediate ssha (left) and from REAPER to final FDR4ALT ssha (datation bias correction applied)

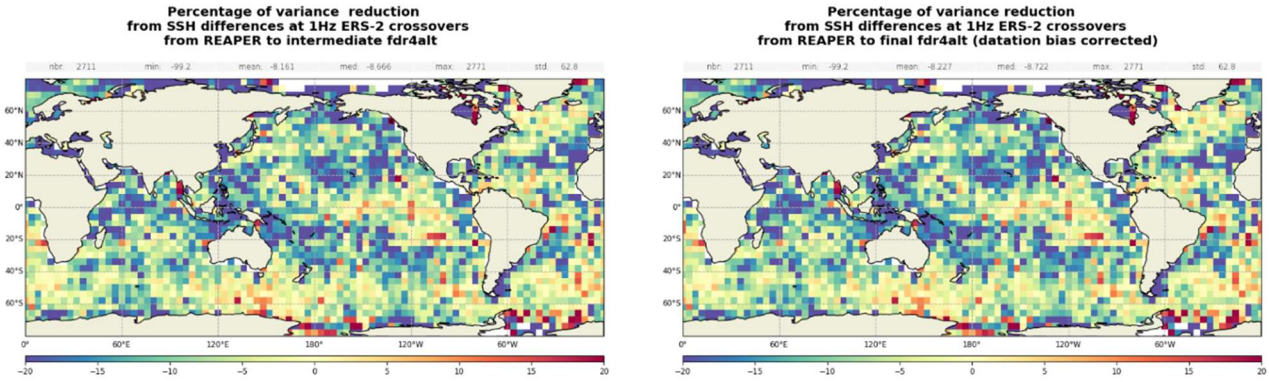

Figure 41: Ocean TDP. Maps of variance reduction at crossovers (1hz dataset) for ERS-2 cycles 1 to 85, from REAPER to intermediate ssha (left) and from REAPER to final FDR4ALT ssha (datation bias correction applied)

3.4.6 Spectra, and noise analysis

Spectra have been calculated on the three datasets for the whole SLA (right part of Figure 42) and for Orbit - Range – MSS (left part of Figure 42). As concerned ERS-2, there is no white noise plateau, instead a red noise is visible. The updated datasets spectrum (in green and red) are slightly under the reference's one, probably thanks to the update of mean sea surface from CLS01 (referenced over 7 years of altimetry data) to the most

recent (referenced over 20 years data). A stange behaviour is visible as a peak over the spectral dump and is not understanding yet.

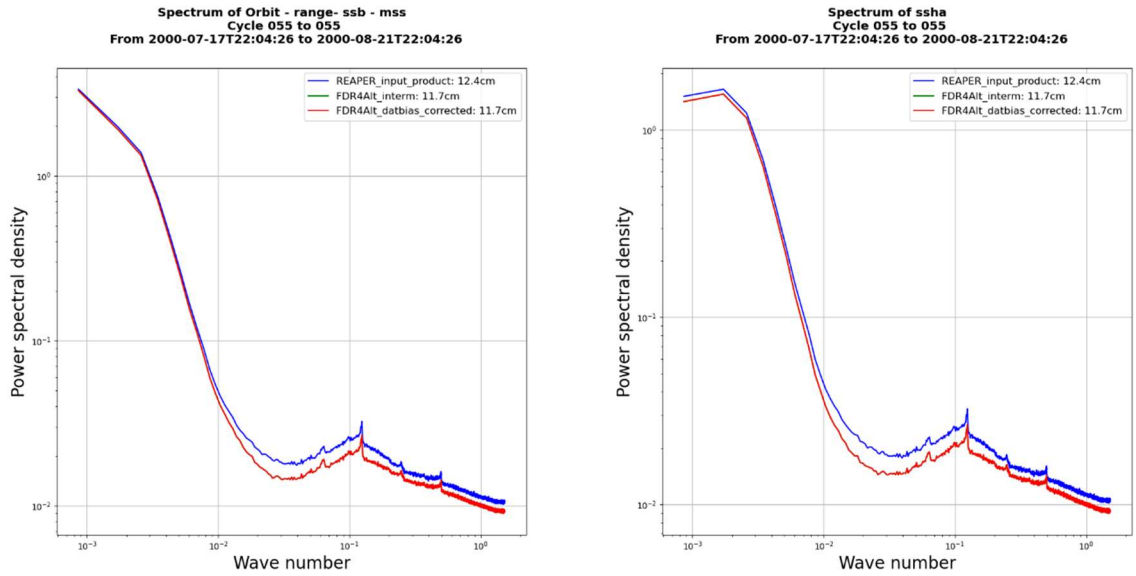

Figure 42: Ocean TDP. (orbit - range - MSS) [left] and SLA [right] spectra over ERS-2 cycle 55

3.4.7 Global Mean Sea Level trend estimation

GMSL estimations have been computed for each 1Hz dataset and compared to TOPEX.

As shown in Figure 43, for the recommended period, FDR4ALT final dataset's trend (2.75mm/year) is closer to TOPEX's (3.23 mm/year) than REAPERS's (1.79 mm/year) or L2P2021's (2.32mm/year).

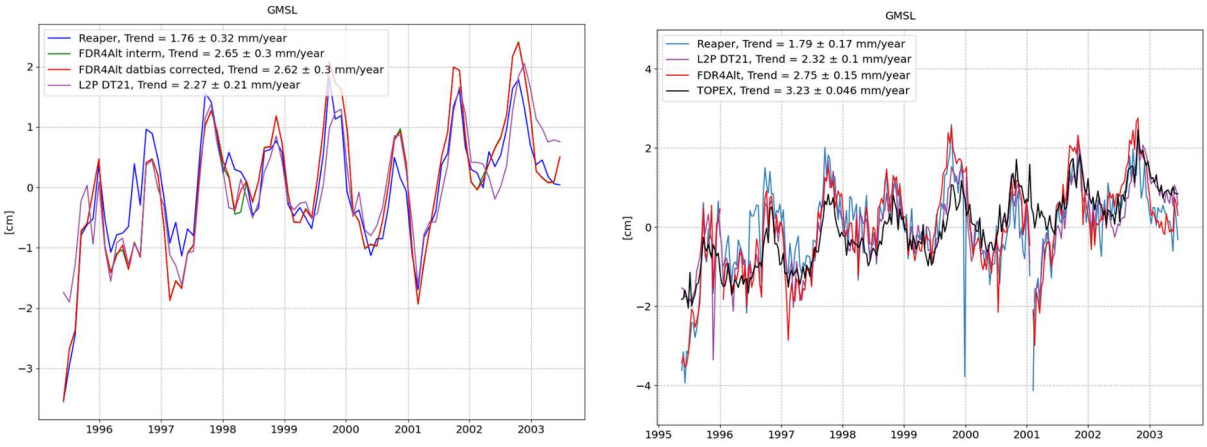

Figure 43: Ocean TDP. GMSL over the whole series and including all ERS latitudes coverage (left), and comparison to TOPEX L2P series, selecting only |latitude|<66° (right)

3.4.8 Conclusions on ERS datasets.

The provided dataset for ERS missions allows to provide a SSHA estimations according to the up-to-date geophysical corrections. In addition, an empirical correction has been applied to take into account a datation bias that was detected on the REAPER-V2 data version. Some improvements could be done:

- ✓ A first improvement on these data could be to understand the origin and correct the datation bias.
- ✓ The compression from 20Hz to 1Hz database step has to be reprocessed, avoiding duplicated points.
- ✓ A new ice detection flag could be used to improve the validation process.
- ✓ A new sea state bias table, adapted to the SSH could improve the 20Hz corrected dataset (the provided dataset has been computed using the 1Hz sea state bias values interpolated to 20Hz points)

3.5 Reference documents

RD 1	Ollivier A., Jettou G. (2018). *Envisat V3.0 reprocessing CalVal report.* https://www.aviso.altimetry.fr/fileadmin/documents/calval/validation_report/EN/BilanCalvalRetraitements2017.pdf
RD 2	Soussi, B. (2018). *Handbook V3.0 Envisat.* Retrieved from ESA: https://earth.esa.int/eogateway/documents/20142/37627/Envisat-RA-2-Level-2-Product-Handbook.pdf
RD 3	Pinori, S. (2018). *ENVISAT-1 PRODUCTS SPECIFICATIONS.* Retrieved from ESA: https://earth.esa.int/eogateway/documents/20142/37627/Envisat-RA-2-product-specifications.pdf
RD 4	Ollivier A., Y. N. (2012). Envisat ocean altimeter becoming relevant for Mean Sea Level Trend Studies. *Marine Geodesy Vol 35*
RD 5	Brockley, D. (2014). *REAPER--Product handbook for ERS Altimetry reprocessed products.*
RD 6	Tran N., D. Vandemark, E.D. Zaron, P. Thibaut, G. Dibarboure, and N. Picot (2019): "Assessing the effects of sea-state related errors on the precision of high-rate Jason-3 altimeter sea level data", Advances in Space Research / special issue " 25 Years of Progress in Radar Altimetry", Volume 68, Issue 2, Pages 963-977, https://doi.org/10.1016/j.asr.2019.11.034, 2021

Appendix A - FDR4ALT deliverables

The table below lists all FDR4ALT deliverables with their respective ID number and confidentiality level.

Document	ID	Confidentiality Level
Products Requirements & Format Specifications Document	[D-1-01] [D-2-02]	Public
Roadmap & Product Summary Document	[D-1-02]	Project Internal
Data Requirements Document	[D-1-03]	Project Internal
System Maturity Matrix	[D-1-04]	Project Internal
Examples of products	[D-1-05]	Project Internal
Review Procedure Document	[D-1-06]	Project Internal
Review Data Package	[D-1-07]	Project Internal
Phase 1 Review Report Document	[D-1-08]	Project Internal
Detailed Processing Model Document	[D-2-01]	Public
Round Robin Assessment Report Document	[D-2-03]	Public
Data Production Status Report	[D-3-01]	Project Internal
Final Output Dataset	[D-3-01]	Public
Product Validation Plan	[D-4-01]	Project Internal
Product Validation Report : FDR	[D-4-02a]	Public
Product Validation Report : Sea-Ice TDP	[D-4-02b]	Public
Product Validation Report: Land-Ice TDP	[D-4-02c]	Public
Product Validation Report : Ocean Waves TDP	[D-4-02d]	Public
Product Validation Report : Ocean & Coastal TDP	[D-4-02e]	Public
Product Validation Report: Inland Waters TDP	[D-4-02f]	Public
Product Validation Report: Atmosphere TDP	[D-4-02g]	Public
Uncertainty Characterization Definition Document	[D-5-01]	Project Internal
Uncertainty Characterization Report	[D-5-02]	Public
Product User Guide	[D-5-03]	Public
Completeness Report ALT	[D-7-01]	Public
Completeness Report MWR	[D-7-02]	Public

Table 3 : List of FDR4ALT deliverables

Appendix B - Acronyms

AATSR	Advanced Along-Track Scanning Radiometer
AEM	Airborne electromagnetic
AIR	AIRWAVES2
AVISO	Archivage, Validation et Interprétation des données des Satellites Océanographiques
AMSR-E	Advanced Microwave Scanning Radiometer - Earth Observing System sensor
AMSU-A	Advanced Microwave Sounding Unit-A
ALT	Altimetry
ASSIST	Arctic Shipborne Sea Ice Standardization Too
ATM	Airborne Topographic Mapper
BDHI	Base de datos Hidrologica integrada
BGEP	Beaufort Gyre Exploration Project
CAL	Calibration
CCI	Climate Change Initiative
CFOSAT	Chinese-French Oceanic SATellite
CDS	Copernicus Data Service
CLS	Collecte Localisation Satellite
CMEMS	Copernicus Marine Environment Monitoring Service
CMSAF	Climate Monitoring Satellite Application Facility
CNES	Centre National des Etudes Spatiales
CRREL	Cold Regions Research and Engineering Laboratory
DAHITI	Database for Hydrological Time Series of Inland Waters
DGA	Direccion General de Aguas
ENVISAT	ENVIronment SATellite
EMD	Empirical mode decomposition
EO	Earth Observation
EPS	European Polar System
ERA	ECMWF Re-Analysis
ERS	European Remote-Sensing Satellite
ESA	European Space Agency
ESTEC	European Space Research and Technology Centre
FCDR	Fundamental Climate Data Record
FDR	Fundamental Data Records
FIDUCEO	Fidelity and uncertainty in climate data records from Earth Observations
FMR	Full Mission Reprocessing
FYI	First Year Ice
GEWEX	Global Energy and Water Exchanges
GFO	Geosat Follow-On
GIEMS	Global Inundation Extent from Multi-Satellites
GMSL	Global Mean Sea Level
GNSS	Global Navigation Satellite System
GPM	Global Precipitation Measurement
GRDC	Global Runoff Data Centre
G-REALM	Global Reservoir And Lake Monitor
G-VAP	GEWEX Water Vapour Assessment
HYBAM	HYdro-géochimie du Bassin AMazonien
ICARE	

IGM	Instituto Geografico Militar
IGN	Instituto Geografico Nacional
IMB	Ice Mass Balance
INA	Instituto Nacional de Agua
ISRO	Indian Space Research Organisation
IRPI	Istituto di Ricerca per la Protezione Idrogeologia
IWMI	International Water Management Institute
LEGOS	Laboratoire d'Etudes en Géophysique et Océanographie Spatiales
LIDAR	Ligth Detection And Ranging
LTAN	Local time of the ascending node
LWP	Liquid Water Path
MAC	Multisensor Advanced Climatology
MEAS-SIM	Measure-Simulation
MQE	Mean Quadratic Error
MSSH	Mean Sea Surface Height
MWR	Microwave Radiometer
NASA	National Aeronautics and Space Administration
NE	North East
NN	Neural Network
NPI	Norwegian Polar institute
NWP	Numerical Weather Prediction
NOAA	National Oceanic and Atmospheric Administration
OIB	Operation Ice Bridge
OLC	Open Loop Calibration
OSTST	Oceanography Surface Topography Science Team
POSTEL	Pôle d'Observation des Surfaces continentales par TELEdétection
PTR	Point Target Response
RD	Reference Document
REAPER	Reprocessing of Altimeter Products for ERS
RM	Review Meeting
RSS	Remote Sensing System
SALP	Service d'Altimétrie et de Localisation Précise
SARAL	Satellite with Argos and Altika
SLA	Sea Level Anomaly
SCICEX	Submarine Arctic Science Program
SGDR	Sensor Geophysical Data Record
SHOA	Servicio Hidrografico y Oceanografico de la Armada
SSB	Sea State Bias
SSH	Sea Surface Height
SSM/I	Special sensor microwave/imager
SST	Sea Surface Temperature
SWH	Significant Wave Height
SWIM	Surface Waves Investigation and Monitoring instrument
TAC	Thematic Assembly Center
TB	Température de Brillance (Brightness Temperature)
TDP	Thematic Data Products
TDS	Test Data Set
TFMRA	Threshold First-Maximum Retracker Algorithm
TMR	Topex Microwave Radiometer
TP	Topex/Poseidon

TCWV	Total column water vapour
VCC	Vicarious calibration
VS	Virtual Station
ULS	Upward Looking Sonar
USA	United States of America
USDA	United States Department of Agriculture
WHALES	Wave Height Adaptive Leading Edge Subwaveform
WTC	Wet Tropospheric Correction